



# NOAA Technical Memorandum NMFS

**MARCH 2024**

## **DEVELOPMENT OF METHODS FOR COLLECTING SPECTRAL DATA FROM FOURIER TRANSFORM NEAR-INFRARED SPECTROSCOPY TO AGE THREE SMALL COASTAL PELAGIC SPECIES (PACIFIC SARDINE, PACIFIC MACKEREL, NORTHERN ANCHOVY) IN THE NORTHEAST PACIFIC OCEAN**

Emma Saas<sup>1</sup>, Emmanis Dorval<sup>2</sup>, Dianna L. Porzio<sup>3</sup>, and Brittany D. Schwartzkopf<sup>4\*</sup>

<sup>1</sup> Saltwater Inc., under contract with Southwest Fisheries Science Center, Anchorage, Alaska

<sup>2</sup> Lynker, under contract with Southwest Fisheries Science Center, Leesburg, Virginia

<sup>3</sup> California Department of Fish and Wildlife, Marine Region, San Pedro, California

<sup>4</sup> NOAA Southwest Fisheries Science Center

Fisheries Resources Division, La Jolla, California

\* corresponding author

NOAA-TM-NMFS-SWFSC-694

U.S. DEPARTMENT OF COMMERCE  
National Oceanic and Atmospheric Administration  
National Marine Fisheries Service  
Southwest Fisheries Science Center

## **About the NOAA Technical Memorandum series**

The National Oceanic and Atmospheric Administration (NOAA), organized in 1970, has evolved into an agency which establishes national policies and manages and conserves our oceanic, coastal, and atmospheric resources. An organizational element within NOAA, the Office of Fisheries is responsible for fisheries policy and the direction of the National Marine Fisheries Service (NMFS).

In addition to its formal publications, the NMFS uses the NOAA Technical Memorandum series to issue informal scientific and technical publications when complete formal review and editorial processing are not appropriate or feasible. Documents within this series, however, reflect sound professional work and may be referenced in the formal scientific and technical literature.

SWFSC Technical Memorandums are available online at the following websites:

SWFSC: <https://swfsc-publications.fisheries.noaa.gov/>

NOAA Repository: <https://repository.library.noaa.gov/>

## **Accessibility information**

NOAA Fisheries Southwest Fisheries Science Center (SWFSC) is committed to making our publications and supporting electronic documents accessible to individuals of all abilities. The complexity of some of SWFSC's publications, information, data, and products may make access difficult for some. If you encounter material in this document that you cannot access or use, please contact us so that we may assist you.  
Phone: 858-546-7000

## **Recommended citation**

Saas, Emma, Emmanis Dorval, Dianna L. Porzio, and Brittany D. Schwartzkopf. 2024. Development of methods for collecting spectral data from Fourier transform near-infrared spectroscopy to age three small coastal pelagic species (Pacific Sardine, Pacific Mackerel, Northern Anchovy) in the northeast Pacific Ocean. U.S. Department of Commerce, NOAA Technical Memorandum NMFS-SWFSC-694.  
<https://doi.org/10.25923/gp34-z216>

**Development of methods for collecting spectral data from Fourier transform near-infrared spectroscopy to age three small coastal pelagic species (Pacific Sardine, Pacific Mackerel, Northern Anchovy) in the northeast Pacific Ocean**

Emma Saas<sup>1</sup>, Emmanis Dorval<sup>2</sup>, Dianna L. Porzio<sup>3</sup>, Brittany D. Schwartzkopf<sup>4\*</sup>

<sup>1</sup>Saltwater Inc., under contract with Southwest Fisheries Science Center, 733 N Street,  
Anchorage, AK 99501

<sup>2</sup>Lynker, under contract with Southwest Fisheries Science Center, 202 Church St., SE / #536,  
Leesburg, VA 20175

<sup>3</sup>California Department of Fish and Wildlife, Marine Region, 2451 Signal Street, AltaSea Berth  
59, San Pedro, CA 90731

<sup>4</sup>Fisheries Resources Division, Southwest Fisheries Science Center  
NOAA National Marine Fisheries Service  
8901 La Jolla Shores Dr., La Jolla, CA 92037

\*corresponding author

Abstract	3
1. Introduction	4
2. Methods	8
2.1 Sample collection	8
2.2 Traditional ageing	9
2.3 Spectral Data Acquisition	11
2.4 Experimental Trials	11
2.4.1 Trial I- Otolith orientation and placement	13
2.4.2 Trial II-Otolith selection and condition	14
2.4.3 Trial III - Spectrometer comparison within and between laboratories	15
2.4.4 Trial IV- Among Accessory Comparison	16
2.5 Analysis and calibration model development	17
2.5.1 Experimental trials	17
2.5.2 Calibration model development	18
3. Results	19
3.1 Experimental Trials	19
3.1.1 Trial I-Otolith orientation and placement	19
3.1.2 Trial II- Otolith selection and condition	21
3.1.3 Trial III - Spectrometer comparison within and between laboratories	22
3.1.4 Trial IV- Among Accessory Comparison	25
3.1.4.1 Pacific Sardine	26
3.1.4.2 Pacific Mackerel	28
3.1.4.3 Northern Anchovy	30
3.2 Calibration models	32
3.2.1 Pacific Sardine	32
3.2.2 Pacific Mackerel	34
3.2.3 Northern Anchovy	35
4. Discussion	37
5. Acknowledgements	39
6. References	40

## Abstract

Methods were developed using Fourier transform near-infrared spectroscopy (FT-NIRS) to acquire spectral data from otoliths of three coastal pelagic species collected in the California Current ecosystem: Pacific Sardine *Sardinops sagax*, Pacific Mackerel *Scomber japonicus*, and Northern Anchovy *Engraulis mordax*. FT-NIRS spectral data were used to build calibration models to evaluate fish-age prediction capabilities and the potential use of ages produced from FT-NIRS in stock assessments. A key challenge of these three species was the light weight of their otoliths (< 1 g) throughout their lifespan, which results in a narrow gradient of otolith weight vs. age. Four experimental trials were conducted to assess the effects of otolith condition, presentation on the spectrometer, choice of spectrometer and scanning technicians, and spectrometer accessories on the quality of spectral output (i.e., absorbance at each wavelength). Spectral data from otoliths were collected using nine accessory set-ups, such as a chrome ring and a Teflon disc, to investigate what procedures would best accommodate the small otolith size. By comparing paired and control otolith output for variation among individuals, we recommended the use of whole and clean otoliths for optimal spectral acquisition. We found that otoliths must be placed in a consistent orientation and location on the quartz sample window of the spectrometer. A chrome ring that reduces the sample window's area provided the optimal spectral data for Pacific Sardine, Pacific Mackerel, and Northern Anchovy otoliths. Compared to other methods, the chrome ring method provided more reproducible spectral outputs within and between technicians when the same spectrometer was used. Using the Savitzky-Golay first derivative filter with 17 smoothing points, the FT-NIRS calibration models developed for Pacific Sardine ( $n = 537$ ) had a multiple coefficient of determination ( $R^2$ ) of 0.83, and residual prediction deviation (RPD) of 2.48, whereas estimates of these parameters were lower for Pacific Mackerel ( $n = 278$ ,  $R^2 = 0.71$ , RPD = 1.91), and Northern Anchovy ( $n = 332$ ,  $R^2 = 0.69$ , RPD = 1.89). These results showed the calibration model for Pacific Sardine performed better than those for Pacific Mackerel and Northern Anchovy, although testing of the prediction models with additional datasets and more rigorous model testing and optimization is required to quantify the accuracy and precision of ages estimated from the FT-NIRS methodology for these three species.

## 1. Introduction

Managing fish stocks is important to ensure their sustainable production over time and maintain ecological function of the population/species. Age-structured models are one of the primary tools used to estimate recruitment, exploitation rate, and abundance among other management parameters (Hilborn and Walters, 1992). Age-structured models include age data, which provides demographic information to reconstruct past and current stock status and forecast critical parameters such as recruitment and biomass under fishing exploitation and management (e.g., Francis, 2016). As of 2013, at least 61 fish stocks worldwide are assessed using Stock Synthesis (SS), a popular statistical age-structured population modeling framework (Methot and Wetzel, 2013). This number is likely much higher at present as 200 stocks are currently assessed in the U.S. alone, using SS and/or other modeling approaches (Methot and Wetzel 2023). The extensive use of age-structured stock assessments makes accurate age estimates a key aspect of fisheries management. Inaccurate age estimates can impede understanding of recruitment variability and bias estimates of mortality, survivorship, stock biomass, spawning-stock biomass, and fishery indices such as catch-at-age (Reeves, 2003; Bertignac and de Pontual, 2007; Yule et al., 2008), which can propagate throughout stock assessments and lead to inaccurate recommendations for managers.

Otoliths are the primary hard structures used for estimating age and growth of marine fishes for most age-structured stock assessments (Secor et al., 1995). Otoliths are inner-ear structures that contribute to hearing and vestibular processes (Lowenstein, 1936). The three otolith pairs that occur in teleost fish are the asterisci, lapilli, and sagittae, with sagittae being the largest and most often used for ageing (Campana and Neilson, 1985). Otoliths are composed of permanent increment deposits (i.e., no reabsorption or remineralization) of protein and aragonite (a polymorph of calcium carbonate,  $\text{CaCO}_3$ ) that manifest on a seasonal timescale as alternating increments of opaque and translucent material creating visible ring-like boundaries called annuli, which researchers use to track fish age and growth throughout their lifetime (Campana and Neilson, 1985; Beckman and Wilson, 1995; Campana, 1999; Passerotti et al., 2022). By weight, otoliths are > 90% mineral, predominantly  $\text{CaCO}_3$ , and the remaining <10% consists of a protein matrix and small amounts of trace elements (Campana, 1999; Payan et al., 2004; Sohn et al., 2005; Chang and Geffen, 2013). The deposition of both the protein matrix and trace elements vary temporally and structurally across the otolith (Hüssy et al., 2004; Thomas et al., 2020).

Otoliths are processed and aged using various techniques including whole otolith surface reading, break-and-burn, and sectioning; the choice of a method is species specific and based on otolith morphology and life history characteristics (Secor et al., 1992). Regardless of the processing technique used, fish age is determined by counting the number of paired opaque and translucent growth bands that form an annulus. Visually, an annulus is defined as the interface between an inner translucent growth increment and the successive outer opaque growth increment (Collins and Spratt, 1969; Yaremko, 1996; Schwartzkopf et al., 2022). For longer-lived species with large and thick otoliths (e.g., rockfishes *Sebastes* spp., Walleye Pollock *Theragra chalcogramma*), break-and-burn or sectioning processing techniques are commonly used (Beamish and McFarlane, 1995; Secor et al., 1995). Conversely, for short-lived species with small and thin otoliths (e.g., Pacific Sardine *Sardinops sagax*, Northern Anchovy *Engraulis mordax*), whole otolith surface ageing is used (Collins and Spratt, 1969; Yaremko, 1996). Each method has advantages and disadvantages in terms of time, costs, precision, and accuracy of age production. Therefore, selecting an adequate method is important to minimize ageing errors while maintaining the efficiency of the ageing process (Secor et al., 1992; Beamish and McFarlane, 1995; Begg et al., 2005).

The annual ageing of well over 1 million fish worldwide underscores the significant allocation of resources dedicated to the ageing process (Campana and Thorrold, 2001), but this is likely an overinvestment in ageing. Generating reliable and accurate ages for stock assessments requires a large investment in time and money by each ageing laboratory. For example, the combined number of otoliths aged by the three largest NOAA ageing laboratories (i.e., AFSC, NEFSC, and NWFSC) in one year can total around 130,000, but the number of otoliths that can be processed and aged in one day varies depending on the species (Lambert et al., 2017). For some groundfish species (e.g., rockfishes, Walleye Pollock, Pacific Hake *Merluccius productus*, Haddock *Melanogrammus aeglefinus*), around 20 to 50 otoliths on average can be processed and aged in a day (J. Short, AFSC, pers. comm.; Lambert et al., 2017; Siskey et al., 2023). With the continued need for age data to assess fish stocks, coupled with static NMFS budgets yet increasing inflation, meeting capacity demands is becoming increasingly difficult, thus there is a need for innovative approaches to determine fish ages.

One innovative approach that is being evaluated to rapidly age fish is Fourier transform near-infrared spectroscopy (FT-NIRS). FT-NIRS is a non-destructive analytical technique that

collects information on the chemical characteristics/composition of a sample via light absorption within the near-infrared electromagnetic spectrum (800 - 2,500 nm). Specifically, this near-infrared spectrum records vibrations from C-H, N-H, and O-H functional groups, and thus is especially informative about organic material. The resulting spectra from FT-NIRS data collected from otoliths show the overall interactions between near infrared light and the molecular composition of the otolith. Passerotti et al. (2022) found that protein concentration may increase and CaCO<sub>3</sub> concentration may decrease in Red Snapper *Lutjanus campechanus* otoliths as fish age increases. Work to further characterize otolith protein composition is ongoing and likely requires analysis on a species-specific basis, as otoliths from different species have unique morphologies, growth patterns, and seem to contain varying proteins (Murayama et al., 2002; Weigele et al., 2016; Passerotti et al., 2022). Though morphology and mass both impact spectral output, compositional changes in otoliths may be an important driver of age prediction (Passerotti et al., 2022). The technology itself has been well established for certifying the chemical composition of liquid and solid foods in the dairy and agricultural industry for decades (Rasco et al., 1991; Sorvaniemi et al., 1993); however, its use in fisheries research is still relatively novel. The research and development for implementation of FT-NIRS at the six NOAA Fisheries Science Centers is part of a NOAA Fisheries strategic initiative (Helser et al., 2019b). The initiative funds research to evaluate FT-NIRS primarily as a rapid method for predicting fish age, to develop methodology for assessed fish species of interest at each center, and to potentially make FT-NIRS ready for practical use on a regular basis in fisheries management. FT-NIRS is also being evaluated by some NOAA Fisheries Science Centers for other applications, such as cryptic species discrimination (Dahl et al., 2024).

Despite lingering ambiguity about the exact mechanisms that underly FT-NIRS age prediction from otoliths, recent studies have started to provide evidence about the potential application of FT-NIRS for fish ageing. FT-NIRS has been shown to reproduce age data directly from traditional ages for several species with relatively good accuracy (i.e., compared to traditional ageing methods), including Walleye Pollock (Helser et al., 2019a; Benson et al., 2023), Red Snapper (Passerotti et al., 2020a; Passerotti et al., 2020b), Saddletail Snapper *Lutjanus malabaricus* (Wedding et al., 2014; Robins et al., 2015), Pacific Cod *Gadus macrocephalus* (Healy et al., 2021), longnose skate *Raja rhina* (Arrington et al., 2022), and Barramundi *Lates calcarifer* (Wright et al., 2021). Additionally, FT-NIRS has been used to

address questions regarding fish reproductive and physiological status, such as salmon maturity (Hampton et al., 2002) and juvenile Pacific cod body and tissue condition (Goldstein et al., 2021). The methods for data collection for the aforementioned species include placing the otoliths convex side down at a consistent orientation, but vary slightly in the accessories used. Helser et al. (2019a) and Passerotti et al. (2020a, 2020b) used a gold-coated reflector (i.e., stamp) over the otolith, though Passerotti et al. (2020b) found the additional use of a Teflon disc improved age prediction models for small sized otoliths. Wedding et al. (2014) placed their samples in quartz glass vials, and Robins et al. (2015) used no accessories at all. The use of accessories, therefore, likely needs to be examined for each new species to be aged using FT-NIRS.

Coastal pelagic species (CPS) are schooling fishes associated with pelagic habitats and occur in both coastal and open ocean waters (Allen et al., 2006). In the California Current Ecosystem, CPS include the finfishes Pacific Sardine, Pacific Mackerel *Scomber japonicus*, Jack Mackerel *Trachurus symmetricus*, and Northern Anchovy. Although all four finfish are included in the Coastal Pelagic Species Fishery Management Plan (PFMC 2019), stock assessments are currently conducted on Pacific Sardine, Pacific Mackerel, and Northern Anchovy stocks (Kuriyama et al., 2020; Kuriyama et al., 2022; Kuriyama et al., 2023). Pacific Sardine and Pacific Mackerel range from southeast Alaska down to southern Baja California, Mexico (Kuriyama et al., 2022; Kuriyama et al., 2023), whereas Northern Anchovy range from northern British Columbia, Canada, to southern Baja California, Mexico (Kuriyama et al., 2022). Pacific Sardine can grow up to about 41 cm standard length (SL) (Eschmeyer et al., 1983), though individuals caught in the fishery are most frequently under 30 cm SL (Kuriyama et al., 2022). Pacific Mackerel can grow up to 63 cm in fork length (FL), but most fish caught in the CPS fishery are less than 45 cm FL (Kuriyama et al., 2023). Northern Anchovy can grow up to 19.7 cm SL but are usually smaller than 15.3 cm SL (Baxter, 1967; Kuriyama et al., 2022; Schwartzkopf et al., 2022). All three species are short-lived, with Northern Anchovy only living up to 7 years, and Pacific Sardine and Pacific Mackerel living up to 15 and 14 years, respectively, with individual fish of less than 5 years old dominating the catch of all three species in recent decades (Kuriyama et al., 2020; Kuriyama et al., 2022; Kuriyama et al., 2023).

Historically, CPS have been an important part of commercial and recreational fisheries along the northeast Pacific coast and have been caught for human consumption, live and dead

bait, and reduction to oil and fish meal for hatcheries (PFMC 2022). For example, from 2011-2014, Pacific Sardine landings were valued at \$14.8 million to the fishery, and at one point export values exceeded \$40 million (PFMC 2022), although the directed fishery has been closed since July 2015 following a large decline in stock biomass (Kuriyama et al., 2020). CPS are also an important part of the food web as prey for marine mammals, seabirds, salmon, sharks, tunas, and many other species (Koehn et al., 2017; Thompson et al., 2019).

Pacific Sardine, Pacific Mackerel, and Northern Anchovy were chosen for evaluation of FT-NIRS because they are federally managed species that are assessed using age data and have a significant workload involved in ageing thousands of otolith pairs each year for assessments. These three CPS present unique challenges to FT-NIRS due to their short lifespans and small size in terms of weight and length of otoliths throughout their lifespan. In this study, we developed a methodology that produces the most informative spectra from these three CPS by evaluating the result of four experimental trials conducted on: 1) otolith orientation and placement on the quartz window of the spectrometer; 2) otolith condition at the time of FT-NIRS processing; 3) comparisons between two difference machines and two different scanning technicians; and 4) the accessories needed to capture the optimal information. Method evaluation was done both qualitatively using graphical comparisons and quantitatively by developing calibration models for each experimental trial.

## **2. Methods**

### 2.1 Sample collection

Samples of Pacific Sardine, Pacific Mackerel and Northern Anchovy were collected from Vancouver Island, British Columbia, Canada to around San Diego, California, with a southernmost boundary around Punta Baja, Baja California, Mexico. Collections occurred via trawl during CPS spring and summer surveys conducted by the National Oceanic and Atmospheric Administration's Southwest Fisheries Science Center (NOAA-SWFSC) that use an acoustic-trawl method to calculate biomass information and monthly port sampling conducted by California Department of Fish and Wildlife (CDFW), Washington Department of Fish and Wildlife (WDFW), and Oregon Department of Fish and Wildlife (ODFW). Pacific Sardine samples were collected during NOAA-SWFSC CPS surveys between 2004 to 2021 and from

port sampling between 2004 to 2016. All Pacific Sardine samples analyzed were collected in U.S. and Canadian waters and considered to be from the northern subpopulation, based on the most recent habitat model for this species (Zwolinski and Demer, 2023). Pacific Mackerel were collected from summer NOAA-SWFSC CPS surveys from 2012 to 2022, and from monthly port sampling conducted by CDFW from 2008 to 2019. Note that only the 2022 summer trawling comprised Pacific Mackerel collected in both U.S. and Mexican waters. Northern Anchovy were collected from 2015 to 2021 during NOAA-SWFSC CPS surveys, and port sampling conducted by CDFW from 2015 to 2020. All Northern Anchovy samples analyzed were collected off Canada and the U.S., and were considered to be from the northern and central subpopulations. Sagittal otoliths were extracted from each individual fish and stored dried in labeled 5 ml centrifuge tubes during the NOAA-SWFSC CPS survey or in 0.68 ml gelatin capsules during port sampling. The otoliths collected from all three species span a large latitude range and thus likely capture the gamut for size at age. For more details on CPS sampling methods, we refer the reader to Dorval et al. (2022).

In addition, a set of Pacific Sardine otoliths ( $n = 223$ ) was selected and included as ‘known age’ samples in the FT-NIRS analysis from an age validation study conducted for the three species in James et al. (*In Review*). Juvenile Pacific Sardine collected in 2014 and 2015, were chemically marked with oxytetracycline (OTC), and maintained in captivity for up to a year. Sagittal otoliths were extracted after mortality and stored dried in black, labeled 10 ml centrifuge tubes. Experimental samples for Pacific Mackerel and Northern Anchovy are not processed yet, and thus were not included in this study.

## 2.2 Traditional ageing

Pacific Sardine, Pacific Mackerel, and Northern Anchovy otoliths were traditionally aged using the methods described by Yaremko (1996), Fitch (1951), and Collins and Spratt (1969), respectively. Ageing methods for all three species were very similar: whole otoliths were submerged in water against a black background, and the number of annuli on the distal side of the otolith was counted using a dissecting microscope at 25x magnification with reflected light. An annulus was defined as the interface between an inner translucent growth increment and the successive outer opaque growth increment (Yaremko, 1996). The final age was determined by the number of annuli, outer marginal increment, and capture date using a July 1 birthdate for

Pacific Sardine and Pacific Mackerel and June 1 for Northern Anchovy. More details on age determination and age reading errors can be found in Dorval et al. (2013), Dorval et al. (2015), Schwartzkopf et al. (2022), and Snodgrass et al. (2023).

Only otoliths with ages agreed upon by all age readers were chosen for the reference sets to create calibration models for each species. To increase the sample size for older age classes of Pacific Sardine, we included otoliths collected and aged by WDFW, as older Pacific Sardine are more common in the Pacific Northwest (Wolf and Duaghtery, 1961; McFarlane et al., 2005). Among all sources, we aimed to have at least 25 samples per age class for the reference set, but this could not be achieved for older ages that are not frequently caught (Table 1).

**Table 1.** Sample sizes per age class for Pacific Sardine (n = 537), Pacific Mackerel (n = 278), and Northern Anchovy (n = 332) reference sets that were used to create a calibration model. CDFW = California Department of Fish and Wildlife, WDFW = Washington Department of Fish and Wildlife, OTC = oxytetracycline, SWFSC = Southwest Fisheries Science Center.

Species	Source	Age (years)									
		0	1	2	3	4	5	6	7	8	9
Pacific Sardine	CDFW - Fishery	9	13	19	19	9	9	4	3	2	0
	WDFW - Fishery	0	0	0	0	0	0	14	22	10	10
	OTC	92	131	3	0	0	0	0	0	0	0
	SWFSC - Trawl	6	15	20	18	18	17	21	25	28	0
Pacific Mackerel	CDFW - Fishery	25	38	23	14	4	1	2	1	1	0
	SWFSC - Trawl	36	45	40	28	9	11	0	0	0	0
Northern Anchovy	CDFW - Fishery	16	21	22	17	5	2	0	0	0	0
	SWFSC - Trawl	30	32	33	39	43	40	25	6	1	0

### 2.3 Spectral Data Acquisition

For all experimental trials and the process of age estimation described below, spectral data were acquired using a Bruker TANGO-R FT-NIR single-channel spectrometer (2021; Bruker Optics<sup>1</sup>, Ettlingen, Germany; Operating Software OPUS version 8.5, SP1) in the 11,528 to 3,952 cm<sup>-1</sup> wavenumber range. Calibration of the TANGO was automatically performed using an internal gold plate standard. Each individual otolith was manually placed on the quartz window of the spectrometer with the sulcus facing down. For each otolith, 64 individual scans at every 16 cm<sup>-1</sup> of wavenumber were taken and averaged into a final raw absorbance value by the OPUS software. Differences in absorbance value peaks generally correspond to differences in fish age and indicate if methods differ. Primary data collection and analysis were performed at the NOAA-SWFSC in La Jolla, California, with some additional data collection for trials performed to compare spectral data between spectrometers at the NOAA-SWFSC Santa Cruz and La Jolla Laboratories.

### 2.4 Experimental Trials

Four experimental trials were conducted to determine the best sample placement, condition, and accessories for collecting spectral data on CPS otoliths using the FT-NIRS methodology, and to compare otolith spectra between technicians and between spectrometers located at the Santa Cruz and La Jolla Laboratories (Figure 1). Given that all three species have relatively little difference in the size of their otoliths, analyses conducted in each experimental trial were done mostly on Pacific Sardine otoliths. The exceptions to this were Trial 2a and Trial 3 which were completed for all three species. Unless otherwise stated, all trials were done only on the otoliths collected from the NOAA-SWFSC CPS survey, hereafter referred to as either the Pacific Sardine trawl set, Pacific Mackerel trawl set, or the Northern Anchovy trawl set (Table 1).

---

<sup>1</sup>Reference to trade names or businesses does not imply endorsement by the National Marine Fisheries Service, National Oceanic and Atmospheric Administration.

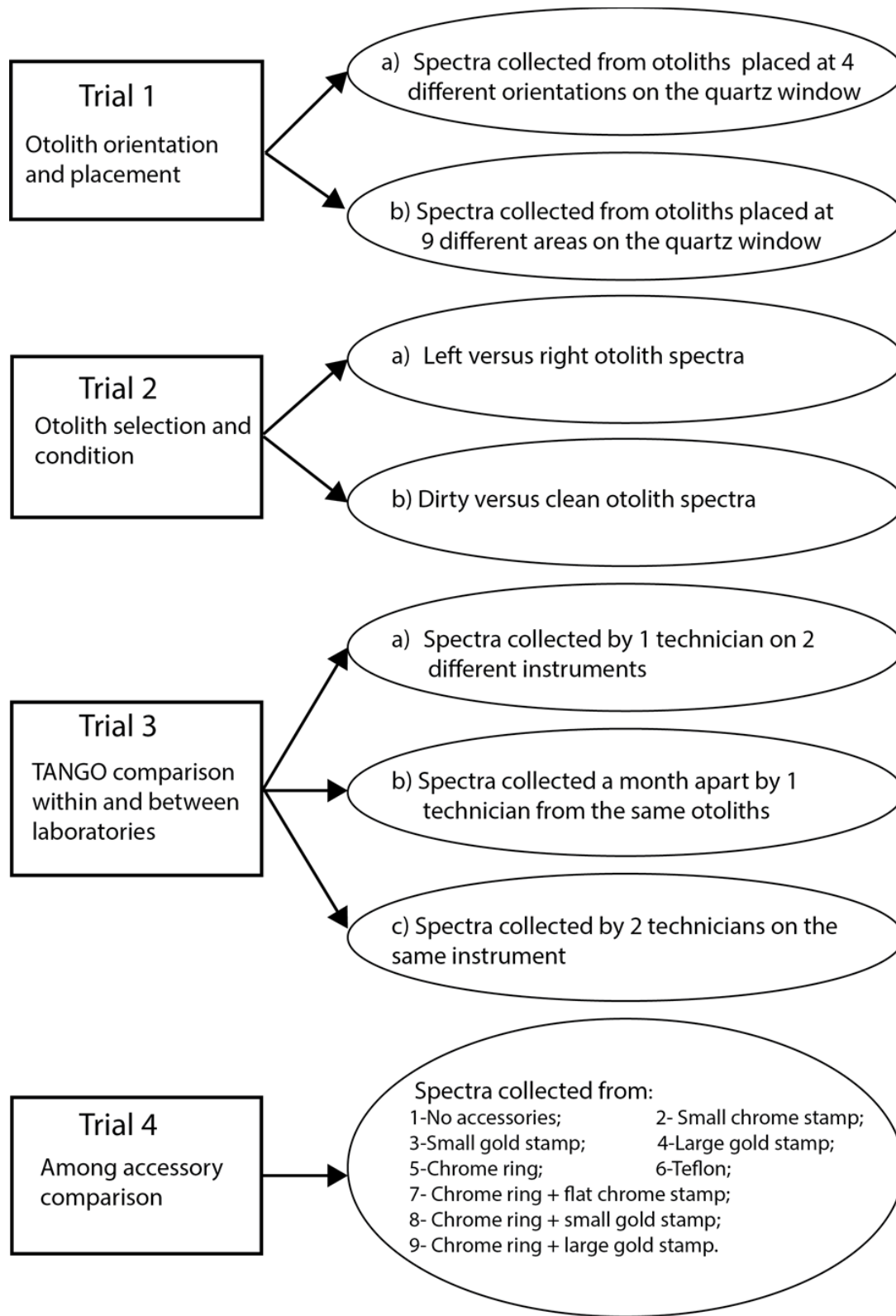


**Figure 1.** A summary of the four experimental trials conducted during this study.

### 2.4.1 Trial I- Otolith orientation and placement

Trial 1a: This experimental trial was conducted to determine the best orientation of the otolith sample on the quartz window. In Trial 1a, one otolith from three individual Pacific Sardine was placed in four different orientations at the center of the window:  $0^\circ$ ,  $90^\circ$ ,  $180^\circ$ ,  $270^\circ$  (Figure 2a).

Trial 1b: This experimental trial was conducted to determine the best position of the otolith on the quartz window. In Trial 1b, those same three Pacific Sardine otoliths were then placed in nine different positions on the window with the  $0^\circ$  orientation (Figure 2b).

Spectral data outputs from Trial 1a and 1b were visually assessed by comparing “usable spectra” versus “non-usable spectra”. We defined ‘usable’ spectra as those that showed minimal noise and a near-flat absorbance signal in the  $\sim 11,528$  to  $7,192$  (or  $>8,000$ ) wavenumber range, with absorbance signal in other areas of the spectrum that falls below 2 absorbance units (AU) on the y-axis due to the limitations of the spectrometer (Jason Erikson, Bruker, pers. comm). In contrast, non-usable spectra were those that deviate from these criteria, showing high noise level, no flat absorbance in the  $\sim 11,528$  to  $7,192$  (or  $>8,000$ ) wavenumber range, and  $AU > 2$  (see Figure 13 “small chrome stamp” for an example of non-usable spectra).

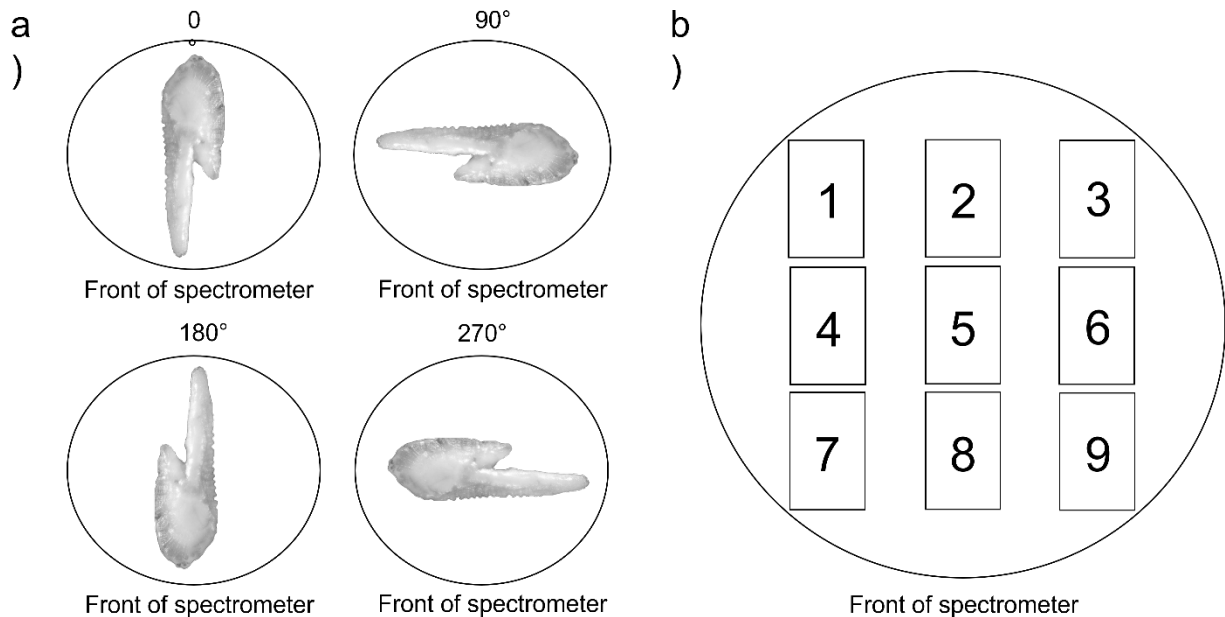


**Figure 2.** a) Otoliths were placed in four orientations,  $0^\circ$ ,  $90^\circ$ ,  $180^\circ$ , and  $270^\circ$ . b) Otoliths were placed in 9 different places on the quartz window. The otoliths shown here are from Pacific Sardine viewed as if you are above the window looking down.

#### *2.4.2 Trial II-Otolith selection and condition*

In this experimental trial, we performed two distinct tests, comparing spectral data between left and right otoliths in Trial 2a, and clean and dirty otoliths in Trial 2b, as described below.

Trial 2a: Left and right otoliths are often of different size (length, width, thickness, and weight) and sometimes they may vary in shape as well. Hence, spectral data collected from left and right otoliths are likely to be different in some species. To test for any potential differences between left and right CPS otoliths, we selected paired-otoliths from 115 Pacific Sardine, 62 Pacific Mackerel, and 68 Northern Anchovy from the trawl samples. Otoliths were placed in the 0° orientation (Figure 2a) in the center of the window (position 5; Figure 2b). For each individual, the left and right otolith were scanned sequentially to minimize any potential machine drift. For each species, calibration models were developed to compare age estimation based on left versus right otoliths.

Trial 2b: Although effort is typically made to clean otolith samples prior to ageing, slightly dirty otoliths often occur in a sample set (Figure 3). Otoliths deemed “dirty” were not completely covered in tissue, but rather had spots of tissue left on the otolith, as this is more commonly seen in archived CPS otoliths than completely dirty samples. Whether these dirty otoliths may affect the spectral data is unknown, hence we compared spectral data collected from “clean otoliths” to “dirty otoliths” to determine whether “dirty otoliths” can provide usable spectral data (i.e., as defined in section 2.4.1). Paired left and right otoliths from 42 Pacific Sardine individuals, where one otolith was dirty and the other was clean, were selected for this analysis. Otoliths were placed in the 0° orientation in the center of the window (position 5; Figure 2b) and then scanned using the TANGO.

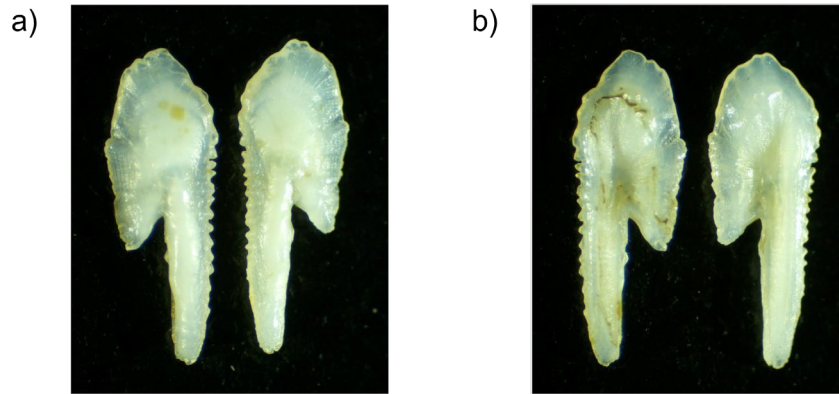


**Figure 3.** a) Distal and b) proximal side of a Pacific Sardine otolith pair, pictured dry. The left otolith was considered ‘dirty’, and the right otolith was considered ‘clean’.

#### *2.4.3 Trial III - Spectrometer comparison within and between laboratories*

In this experimental trial we compared the reproducibility of spectral data between two spectrometers of the same model and specifications, with one spectrometer located at the SWFSC La Jolla lab and the other at the SWFSC Santa Cruz lab (Trial 3a), with the spectrometer at the SWFSC La Jolla lab over time within the same technician (Trial 3b), and between technicians with the spectrometer at the SWFSC La Jolla lab (Trial 3c). Maintaining stable environmental conditions (e.g., atmospheric pressure, air flow, temperature, humidity, light intensity, etc.) in a laboratory is important for the reproducibility of data, and thus using the same spectrometer model and specifications may produce different spectral data at different labs. Similarly, different technicians may have different consistencies in processing and presenting samples to the spectrometer and/or may prefer different environmental conditions while processing samples. The magnitude of these differences is not well understood, and it may vary depending on the size of otoliths being analyzed. For example, less stable environments could have greater impact on smaller otoliths than on larger otoliths, and thus it is important to quantify their potential effects in order to standardize analytical procedures and data within and between laboratories.

Trial 3a: During this trial, technician 1 selected a set of 168 Pacific Sardine otoliths. Then, this technician processed and analyzed these otoliths firstly using the La Jolla lab spectrometer, and secondly the Santa Cruz lab spectrometer. For both spectrometers, the

accessories used were a chrome ring and the La Jolla lab's gold stamp. Note that technician 1 used the same specifications for each spectrometer, but environmental conditions in the two labs were likely different. Spectral data from these two analytical runs were analyzed and then compared based on age estimates from calibration models developed for each lab's spectrometer.

Trial 3b: For this trial, the primary FT-NIRS technician at the La Jolla lab (technician 1) first selected a set of 168 Pacific Sardine otoliths from the trawl samples. Second, technician 1 processed and analyzed these otoliths one month apart using the SWFSC spectrometer. Third, these two analytical runs were compared based on age estimates from calibration models developed for each run.

Trial 3c: The same Pacific Sardine trawl set ( $n = 168$ ) was processed and analyzed by a secondary SWFSC La Jolla technician (technician 2) using the La Jolla spectrometer. Note that technician 2 was trained by technician 1, and both ran the spectrometer with the same specifications.

#### *2.4.4 Trial IV- Among Accessory Comparison*

Accessories, such as a Teflon disc, have been used by past studies investigating the feasibility of FT-NIRS on small otoliths as a means to improve the signal by reducing stray light (Passerotti et al., 2020; 2022). Following this paper, we tried several combinations of accessories to determine which ones, if any, were needed to give the most optimal and repeatable spectral data. The nine combinations of accessories that were tested on five otoliths of Pacific Sardine, five otoliths of Pacific Mackerel, and five otoliths of Northern Anchovy included: 1) no accessory; 2) a small chrome stamp; 3) a small gold stamp; 4) a large gold stamp; 5) a chrome ring; 6) a chrome ring plus a flat chrome stamp; 7) a chrome ring plus a small gold stamp; 8) a chrome ring plus a large gold stamp; and 9) a teflon disc (Figure 4). The flat chrome stamp (Figure 4b), rather than the chrome stamp (Figure 4a), was used in combination with the chrome ring to prevent light from escaping through any gaps. Accessories that resulted in spectra that lacked the above criterion of a "usable" scan were excluded from further testing. Promising methods were scaled up to include a larger subset of otoliths for a calibration model and compared across all three species.

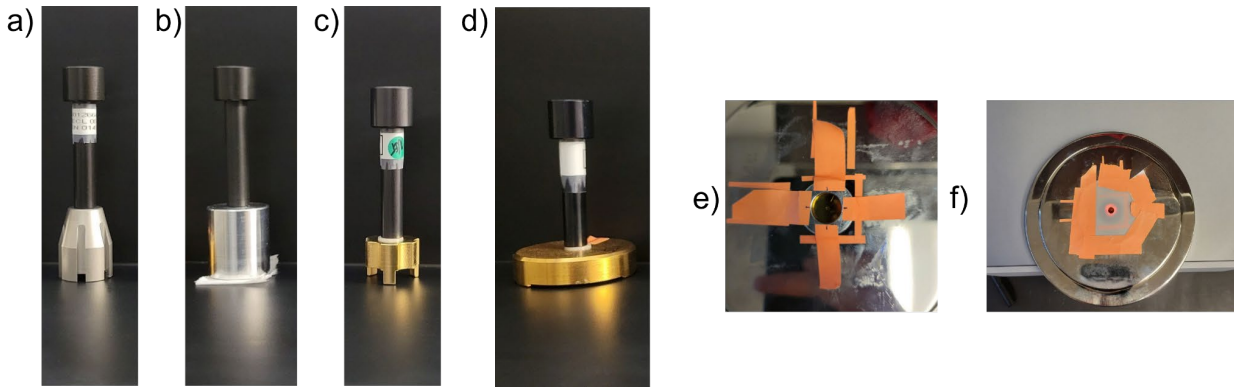


**Figure 4.** The accessories used to test methods, sometimes in conjunction with one another, were a) small chrome stamp, b) flat chrome stamp, c) small gold stamp, d) large gold stamp, e) chrome ring taped to the spectrometer, and f) Teflon disc taped to the spectrometer.

## 2.5 Analysis and calibration model development

Spectra were imported, preprocessed, and analyzed in the R v4.2.1 statistical programming software (R Core Team 2022) with the R packages ‘hyperSpec’ (Beleites and Sergio, 2023), ‘mdatools’ (Kucheryavskiy, 2020), and ‘pls’ (Liland et al., 2022). Congruent with the protocol used by Helser et al. (2019a) and Healy et al. (2021), wavenumbers over 8,000  $\text{cm}^{-1}$  were omitted from all analyses as they yield little relevant information.

### *2.5.1 Experimental trials*

A calibration model was developed for each experimental trial. Spectra were preprocessed using a Savitzky-Golay first derivative with 17 smoothing points (polynomial order = 2) transformation as this has been found to produce the best model results for otolith spectra for multiple species (Helser et al., 2019a; Passerotti et al., 2020b; Healy et al., 2021). Models were produced with a partial least squares regression using the ‘plsr’ function in the ‘pls’ package in R statistical software (Liland et al., 2022) and a leave-one-out (LOO) cross-validation option with a SIMPLS algorithm. Because most experimental trials had a small subset of otoliths, importance was placed on the resulting age estimations from the calibration model and not on the quality of model fit itself. For example, for Trial 2a (left vs. right), a calibration model was built with only the left otoliths, and then another calibration model was built with only the right otoliths for each individual. Resulting age estimates for each sample were then compared between experiments by calculating the Pearson correlation coefficient ( $r$ ) to measure the

strength of the linear relationship between the estimates (i.e., how closely each method produced the equivalent results). Descriptors like “weak”, “moderate” or “strong” relationships have been used to translate the correlation coefficient into a measurable term, but these are arbitrary and inconsistent among studies and fields of study, although a coefficient of  $> 0.9$  is generally agreed upon as a strong relationship (Schober et al., 2018). For this work, we described the correlation as weak for values lower than 0.8, moderate for values between 0.80 and 0.89, strong for values between 0.90 and 0.95, and very strong for values  $> 0.95$ , which is a slight modification from Schober et al. (2018).

### *2.5.2 Calibration model development*

After determining the best otolith placement, condition, and accessory type for each species, a calibration model was developed for age estimations on the full reference set for each species (Table 1) to confirm that the chosen placement and accessory produced an adequate model. The number of external variables was also an important consideration in choosing the final analytical procedure as using the fewest accessories is preferred to maintain long-term consistency (Jason Erikson, Bruker, pers. comm.). Because of this, we created our calibration models for each species using the chrome ring only accessory. We did not choose to use zero accessories as some of the smallest otoliths produced background absorbance values over 2, which violates the Beer-Lambert Law as there is a non-linear relationship between absorbance and concentration after  $\sim 2$  absorbance units, and thus produces non-useable data (Jason Erikson, pers. comm.).

Five data preprocessing treatments were evaluated: 1) No preprocessing, 2) Standard Normal Variate (SNV), 3) Multiplicative Scatter Correction (MSC), 4) Savitzky-Golay first derivative with 17 smoothing points (polynomial order = 2), and 5) Savitzky-Golay second derivative with 17 smoothing points (polynomial order = 2). Goodness of fit was judged based on the coefficient of multiple determination ( $R^2$ ), root mean squared error of cross validation (RMSECV), and residual prediction deviation (RPD) values. In general, RPD values  $> 3$  have excellent predictive ability, between 2 to 3 have limited predictive ability, and  $< 2$  may not have any predictive ability (Liu et al. 2020), but some have deemed RPDs between 1.5 and 2 to have moderate predictive ability (Cohen et al., 2007; D'Acqui et al., 2010).

### 3. Results

#### 3.1 Experimental Trials

##### 3.1.1 Trial I-Otolith orientation and placement

Raw spectra appeared to have baseline shifts among orientations (Trial 1a; Figure 5a), but after preprocessing, spectra appear more similar but still may have slight differences at the peaks (Figure 5b). The placement on the spectrometer window was very important and the resulting raw and preprocessed spectra differed among placement positions (Trial 1b: Figure 6a,b). Having otoliths in placement position 7, 8, or 9 (bottom left, bottom center, bottom right, respectively) produced spectra with almost no prominent peaks, whereas position 5 (center, center) appeared to produce spectra with very prominent peaks, which was an improvement (Figure 6).

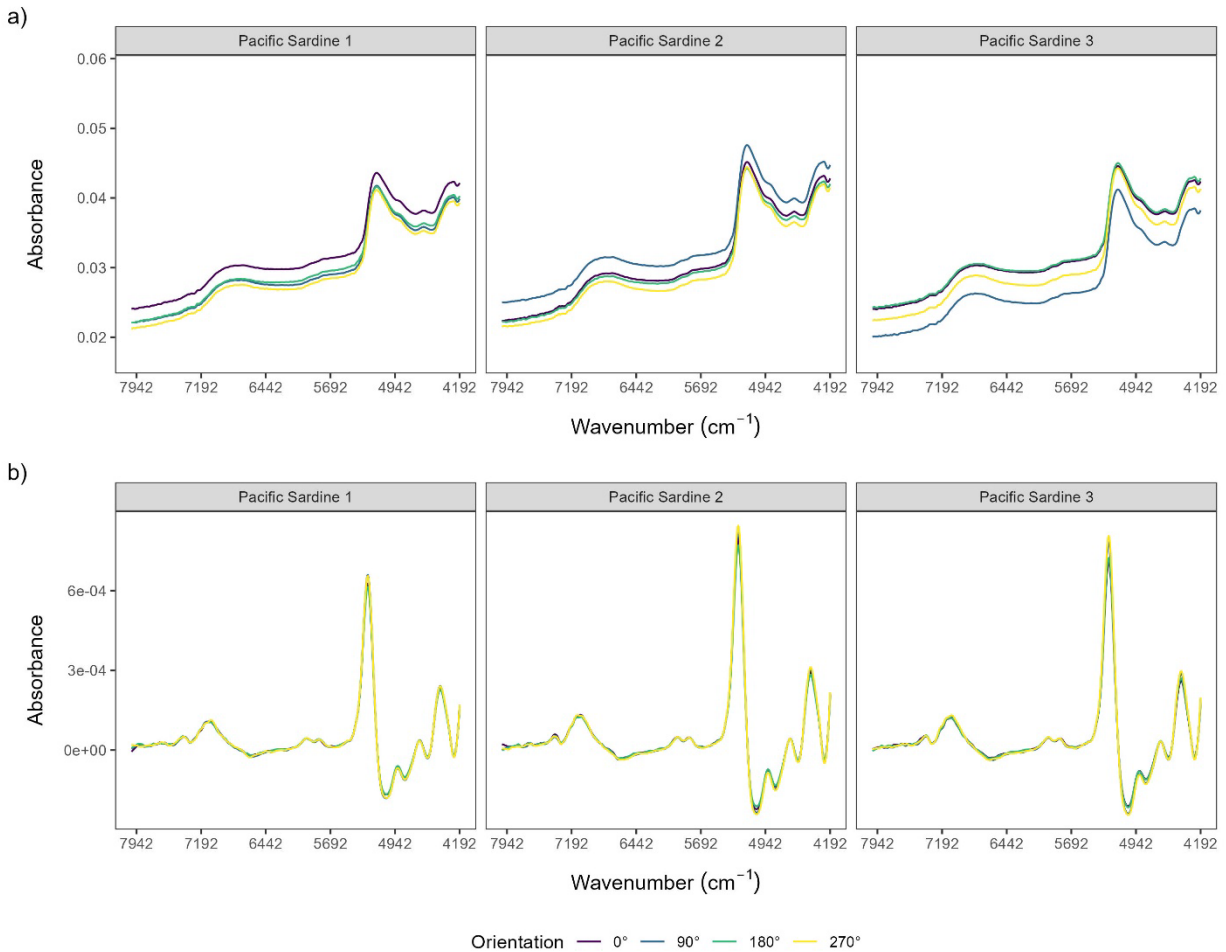


**Figure 5.** a) Raw and b) Savitzky-Golay first derivative with 17 smoothing points (polynomial order = 2) transformed spectra of three Pacific Sardine otoliths in four different orientations. See Figure 2a for what each orientation represents.

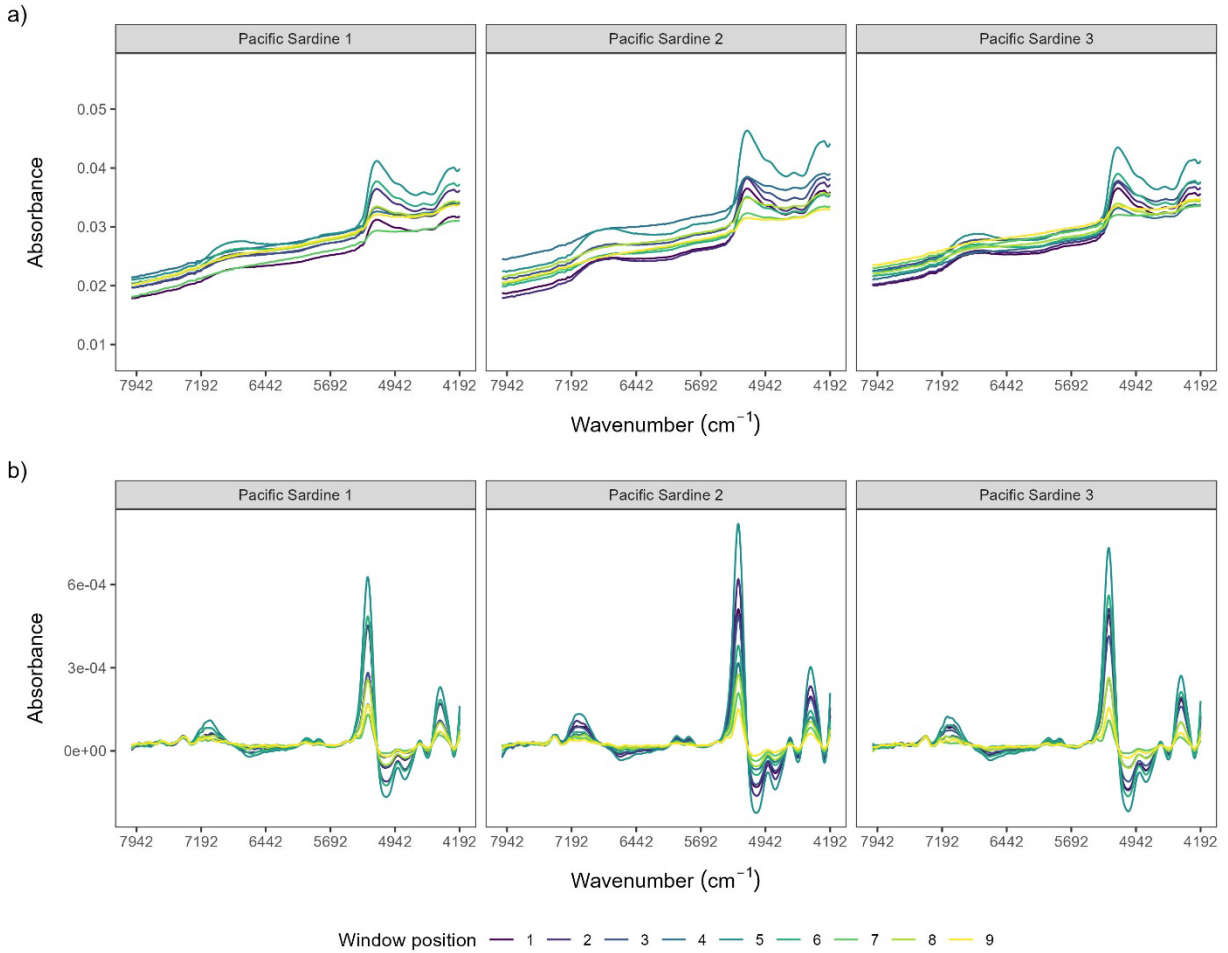


**Figure 6.** a) Raw and b) Savitzky-Golay first derivative with 17 smoothing points (polynomial order = 2) transformed spectra of three Pacific Sardine otoliths in nine different positions on the spectrometer window. See Figure 2b for what each window position represents.

### 3.1.2 Trial II- *Otolith selection and condition*

Age estimations using preprocessed data from left and right otoliths of Pacific Sardine, Pacific Mackerel, and Northern Anchovy showed no substantial differences and had strong or very strong correlations ( $r = 0.97$ ,  $r = 0.99$ ,  $r = 0.95$ , respectively; Trial 2a; Figure 7, see Section 2.5.1 for description of correlation values).

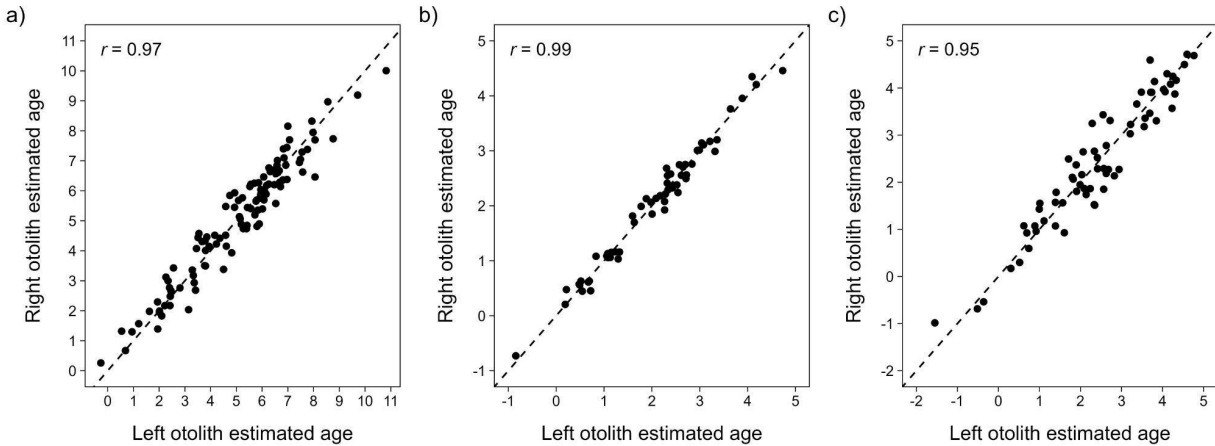


**Figure 7.** Correlations between model age estimations from left and right otoliths, using a subset of: a) the Pacific Sardine trawl set ( $n = 115$ ), b) the Pacific Mackerel trawl set ( $n = 62$ ), and c) the Northern Anchovy trawl set ( $n = 68$ ). The dashed line represents a 1:1 line. The Pearson correlation coefficient ( $r$ ) value is also presented.

Age estimation using preprocessed data from dirty and clean otoliths of the same individual showed little difference and had a very strong correlation ( $r = 0.97$ ; Trial 2b; Figure 8).

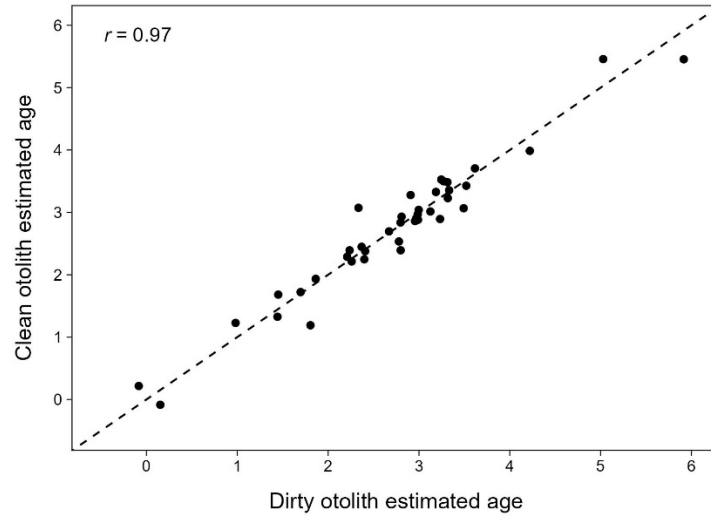


**Figure 8.** Correlation between model age estimations from clean and dirty otoliths using a subset of the Pacific Sardine trawl set ( $n = 42$ ). The dashed line represents a 1:1 line. The Pearson correlation coefficient ( $r$ ) value is also presented.

### 3.1.3 Trial III - Spectrometer comparison within and between laboratories

The Pacific Sardine ages estimated using preprocessed data between spectrometers showed a very strong correlation ( $r = 0.96$ ; Trial 3a; Figure 9). The Pacific Sardine ages estimated a month apart showed a very strong correlation ( $r = 0.97$ ; Trial 3b; Figure 10). The Pacific Sardine ages estimated between technician 1 and technician 2 showed very strong correlation ( $r = 0.99$ ; Trial 3c; Figure 11).

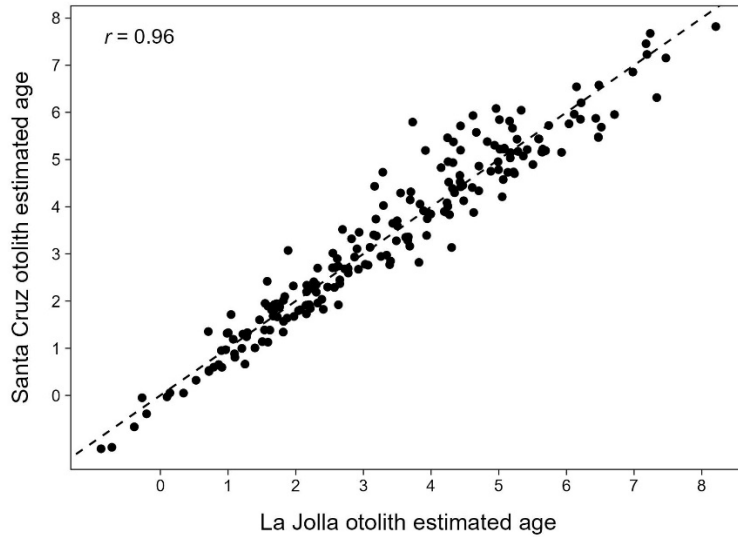


**Figure 9.** Correlation between estimated ages from the spectrometer at the NOAA-SWFSC La Jolla lab and the spectrometer at the NOAA-SWFSC Santa Cruz lab, using the La Jolla lab's gold stamp. All samples were analyzed and processed by technician 1, using a subset of the Pacific Sardine trawl set ( $n = 168$ ). The dashed line represents a 1:1 line. The Pearson correlation coefficient ( $r$ ) value is also presented.

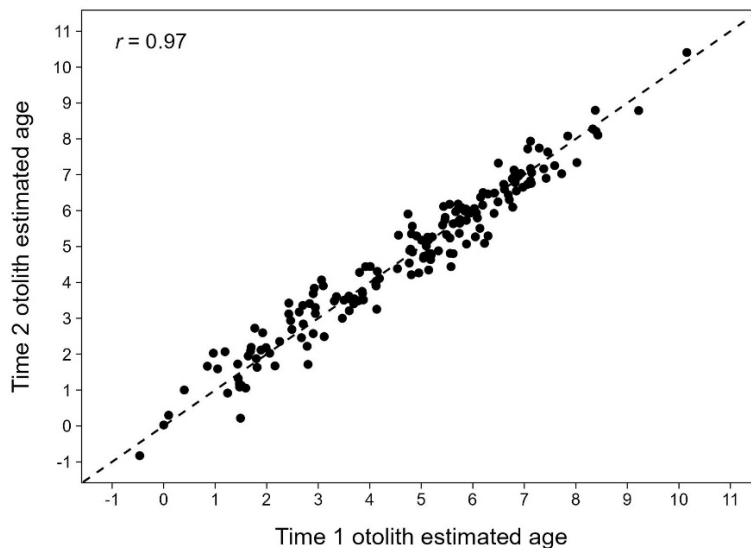


**Figure 10.** Correlation between estimated ages from spectra collected by technician 1 a month apart from the Pacific Sardine trawl set data ( $n = 168$ ) on the spectrometer at the NOAA-SWFSC La Jolla lab one month apart. The dashed line represents a 1:1 line. The Pearson correlation coefficient ( $r$ ) value is also presented.

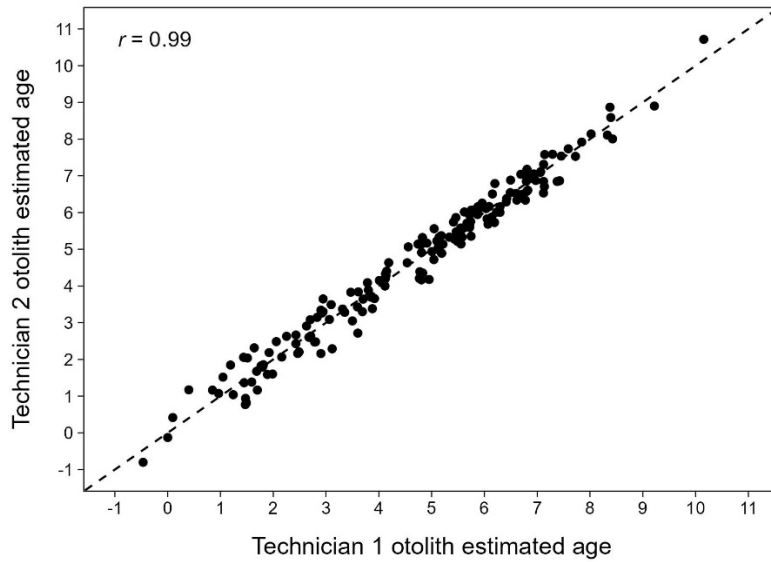


**Figure 11.** Correlation between estimated ages from otolith spectra collected by technicians 1 and 2 from the Pacific Sardine trawl set data ( $n = 168$ ) on the spectrometer at the NOAA-SWFSC La Jolla lab. The dashed line represents a 1:1 line. The Pearson correlation coefficient ( $r$ ) value is also presented.

### 3.1.4 Trial IV- Among Accessory Comparison

The choice of accessory greatly influenced the shape and absorbance values observed for raw spectra for the five Pacific Sardine, Pacific Mackerel, and Northern Anchovy otoliths (Figure 12). The accessories that were completely ruled out for further testing due to a lack of a near-flat background (11,528 to 8,000 wavenumber range) included the small chrome stamp and small gold stamp, with or without the chrome ring, the large gold stamp without a chrome ring, and teflon disc (Figure 13). The three accessories that were chosen for further testing on the trawl set for Pacific Sardine, the fishery set for Pacific Mackerel, and a subset of the trawl set for Northern Anchovy were: 1) no accessory, 2) chrome ring only, and 3) chrome ring + large gold stamp.

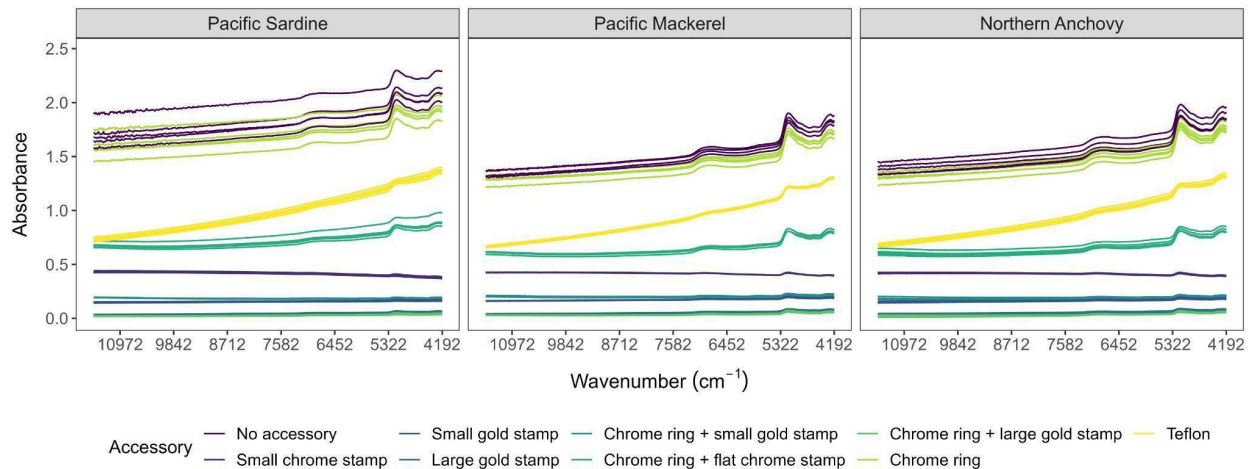


**Figure 12.** Raw spectra of the 9 different accessory combinations for Pacific Sardine, Pacific Mackerel, and Northern anchovy otoliths. This figure is meant to showcase the differences in absorbance values among accessories for each species. See Figure 13 for a zoomed in version of the spectra for each accessory.

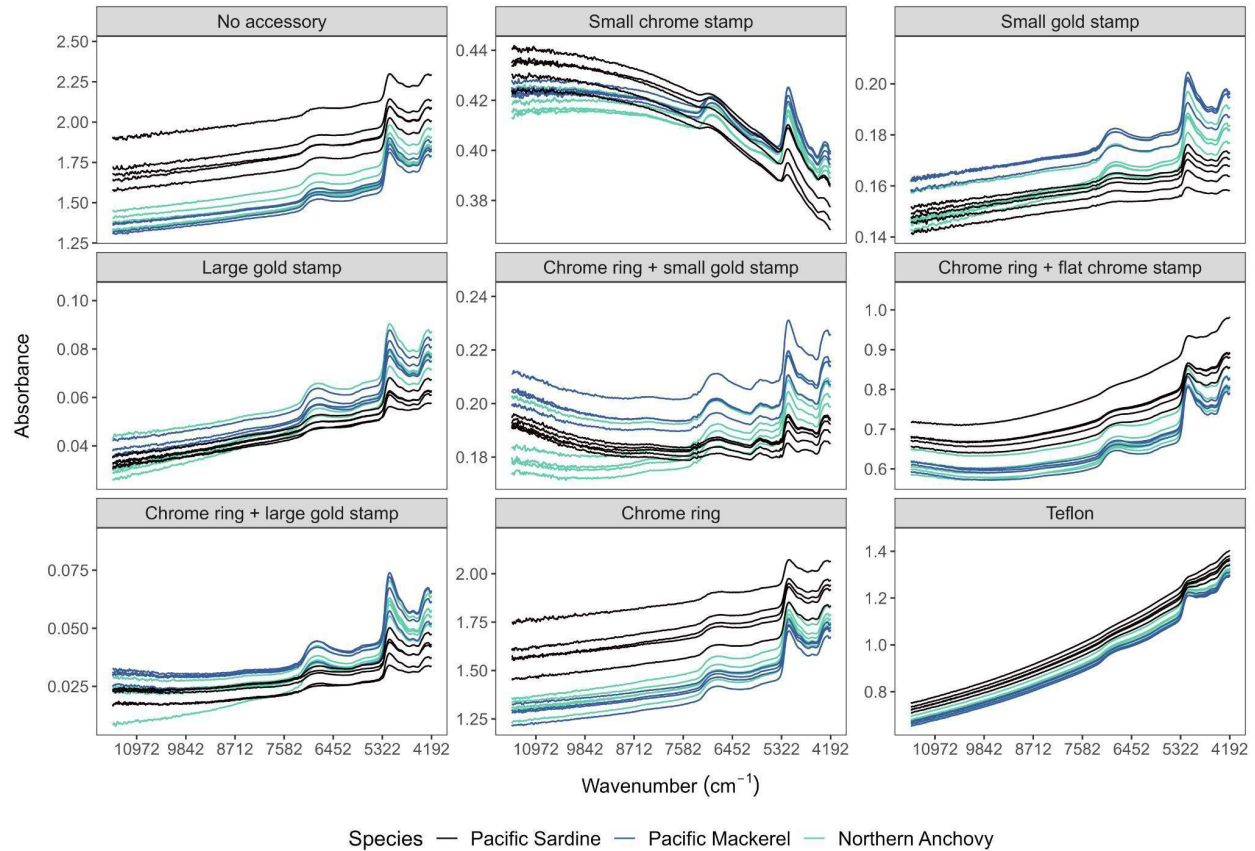


**Figure 13.** Raw spectra of five Pacific Sardine, Pacific Mackerel, and Northern anchovy otoliths for the 9 different accessory combinations. This figure is meant to showcase the different patterns of the raw spectra, so the y-axes are on different scales for each accessory.

#### 3.1.4.1 Pacific Sardine

The best transformation varied among accessories (i.e., no accessory, chrome ring only, and a chrome ring + large gold) (Table 2). The model with the highest RPD was the Savitzky-Golay first derivative with no accessory, but the number of components was large ( $n = 6$ ), which may indicate overfitting. The model with no transformation and with a chrome ring + large gold stamp had the lowest RMSECV, and the prediction power was the second largest among all models ( $RPD = 2.28$ ). When comparing age estimations among accessories using the best transformation per accessory, there was moderate to strong correlation ( $r = 0.92, 0.92, 0.86$ ), with the lowest correlation between chrome ring only and gold stamp + chrome ring ( $r = 0.86$ ; Figure 14).

**Table 2.** Partial least squares regression model output of the Pacific Sardine trawl set (n = 168) for the three accessory types and five transformations. For the transformations, SNV = Standard normal variate, MSC = Multiplicative scattering correction, SG-1 = Savitzky-Golay first derivative, and SG-2 = Savitzky-Golay second derivative. RMSECV = root mean squared error of cross validation, R<sup>2</sup> = coefficient of multiple determination (R<sup>2</sup>), RPD = residual prediction deviation.

<b>Accessory</b>	<b>Transformation</b>	<b>Number of components</b>	<b>RMSECV</b>	<b>R<sup>2</sup></b>	<b>RPD</b>
No accessory	None	5	1.29	0.72	2.00
	SNV	4	1.45	0.65	1.80
	MSC	4	1.45	0.65	1.80
	SG-1	6	1.24	0.74	2.34
	SG-2	2	1.54	0.60	1.68
Chrome ring	None	5	1.33	0.71	1.99
	SNV	4	1.39	0.68	1.86
	MSC	5	1.3	0.72	2.10
	SG-1	4	1.3	0.72	2.02
	SG-2	2	1.41	0.67	1.86
Chrome ring + gold stamp	None	4	1.12	0.79	2.28
	SNV	4	1.17	0.77	2.21
	MSC	4	1.18	0.77	2.20
	SG-1	2	1.17	0.77	2.16
	SG-2	2	1.15	0.78	2.22

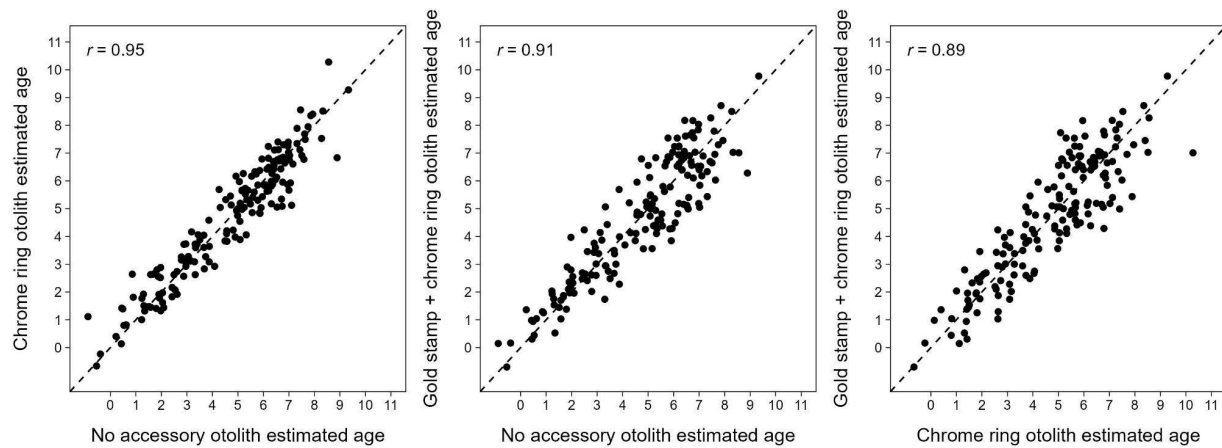


**Figure 14.** Correlations between estimated ages from spectra collected with no accessory, chrome ring only, and chrome ring + large gold stamp on the Pacific Sardine trawl set data ( $n = 168$ ). All spectra were collected by technician 1 on the spectrometer at the NOAA-SWFSC La Jolla. The dashed line represents a 1:1 line. The Pearson correlation coefficient ( $r$ ) value is also presented.

#### 3.1.4.2 Pacific Mackerel

Only the Pacific Mackerel fishery set ( $n = 109$ ) was used to compare the no accessory, chrome ring only, and a chrome ring + large gold stamp accessories. The best transformation varied among accessories, and the no transformation model using the chrome ring + large gold stamp had the lowest RMSECV, highest  $R^2$ , and highest RPD (Table 3). A close second was the model with the Savitzky-Golay first derivative transformation with a chrome ring only as it has the second lowest RMSEP and highest  $R^2$  and RPD, and the number of components was smaller than the best fitting model. When comparing age estimations among accessories using the best model per accessory, there were strong to very strong correlations ( $r = 0.96, 0.94, 0.96$ ; Figure 15).

**Table 3.** Partial least squares regression model output of the Pacific Mackerel fishery set (n = 109) for the three accessory types and five transformations. For the transformations, SNV = Standard normal variate, MSC = Multiplicative scattering correction, SG-1 = Savitzky-Golay first derivative, and SG-2 = Savitzky-Golay second derivative. RMSECV = root mean squared error of cross validation,  $R^2$  = coefficient of multiple determination ( $R^2$ ), RPD = residual prediction deviation.

<b>Accessory</b>	<b>Transformation</b>	<b>Number of components</b>	<b>RMSECV</b>	<b><math>R^2</math></b>	<b>RPD</b>
No accessory	None	3	0.71	0.79	2.33
	SNV	3	0.91	0.64	1.81
	MSC	3	0.91	0.64	1.81
	SG-1	2	0.73	0.77	2.20
	SG-2	1	0.74	0.76	2.13
Chrome ring	None	3	0.71	0.78	2.41
	SNV	3	0.88	0.66	1.85
	MSC	3	0.88	0.66	1.85
	SG-1	3	0.59	0.85	2.80
	SG-2	1	0.71	0.78	2.23
Chrome ring + gold stamp	None	4	0.56	0.866	2.94
	SNV	4	0.70	0.79	2.58
	MSC	3	0.79	0.731	2.07
	SG-1	1	0.62	0.835	2.56
	SG-2	1	0.61	0.839	2.59

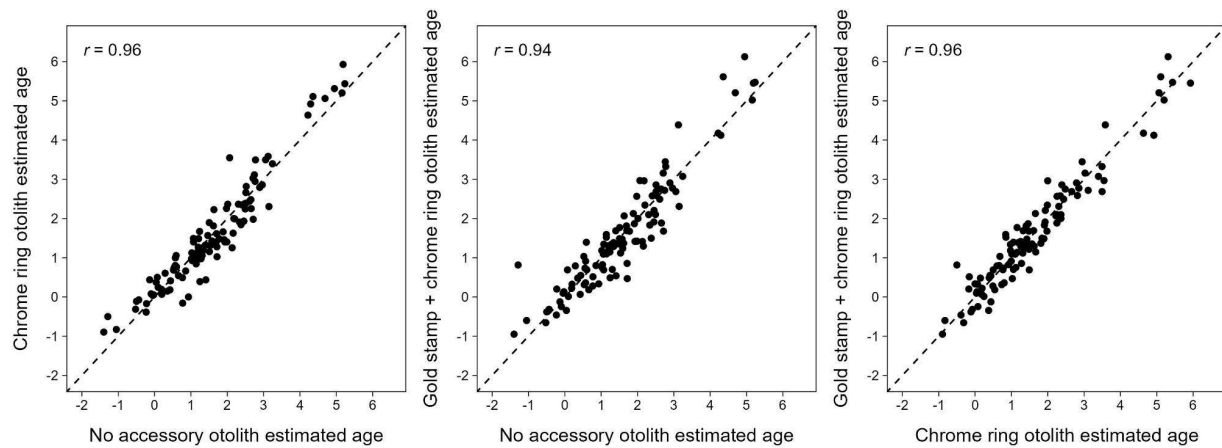


**Figure 15.** Correlation between estimated ages from otolith spectra collected with no accessory, chrome ring only, and chrome ring + large gold stamp on the Pacific Mackerel fishery set ( $n = 109$ ). All spectra were collected by technician 1 on the spectrometer at the NOAA-SWFSC La Jolla lab using. The dashed line represents a 1:1 line. The Pearson correlation coefficient ( $r$ ) value is also presented.

### 3.1.4.3 Northern Anchovy

A subset of the Northern Anchovy trawl set ( $n = 124$ ) was used to compare the no accessory, chrome ring only, and a chrome ring + large gold stamp accessories. The best transformation varied among accessories, and the no transformation model using the chrome ring only had the lowest RMSECV, highest  $R^2$ , and highest RPD (Table 4). When comparing age estimations among accessories using the best model per accessory, there was strong to very strong correlation ( $r = 0.99, 0.92, 0.93$ ), with almost perfect correlation between no accessory and chrome ring only ( $r = 0.99$ ; Figure 16).

**Table 4.** Partial least squares regression model output of a subset of the Northern Anchovy trawl set (n = 124) for the three accessory types and five transformations. For the transformations, SNV = Standard normal variate, MSC = Multiplicative scattering correction, SG-1 = Savitzky-Golay first derivative, and SG-2 = Savitzky-Golay second derivative. RMSEP = root mean squared error of cross validation,  $R^2$  = coefficient of multiple determination ( $R^2$ ), RPD = residual prediction deviation.

<b>Accessory</b>	<b>Transformation</b>	<b>Number of components</b>	<b>RMSECV</b>	<b><math>R^2</math></b>	<b>RPD</b>
No accessory	None	2	1.09	0.53	1.51
	SNV	2	1.22	0.42	1.35
	MSC	2	1.22	0.42	1.35
	SG-1	1	1.20	0.44	1.36
	SG-2	1	1.19	0.45	1.37
Chrome ring	None	2	1.09	0.54	1.51
	SNV	3	1.13	0.50	1.50
	MSC	3	1.13	0.50	1.50
	SG-1	1	1.17	0.46	1.38
	SG-2	1	1.18	0.46	1.38
Chrome ring + gold stamp	None	1	1.15	0.48	1.42
	SNV	3	1.13	0.50	1.49
	MSC	2	1.19	0.44	1.40
	SG-1	1	1.15	0.48	1.42
	SG-2	1	1.15	0.48	1.42

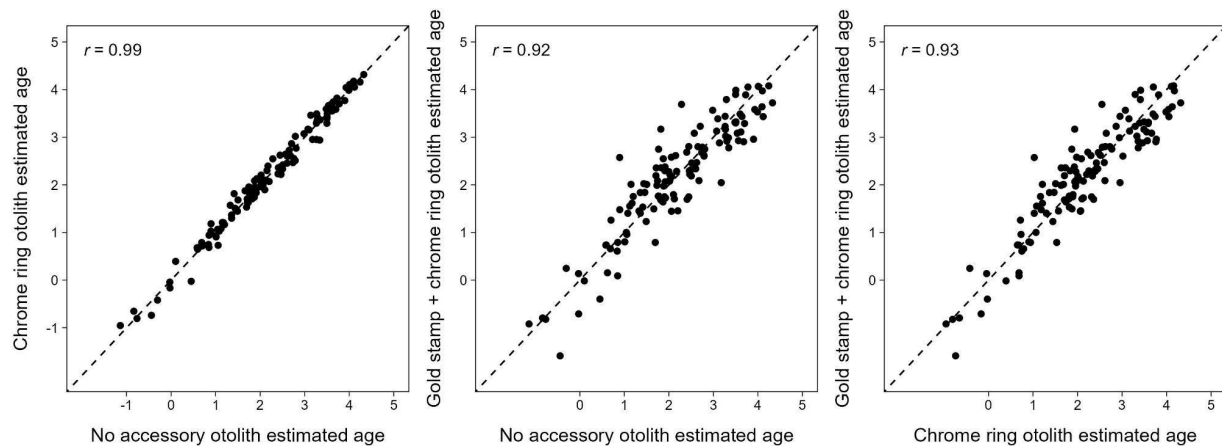


**Figure 16.** Correlations between estimated ages from otolith spectra collected with no accessory, chrome ring only, and chrome ring + large gold stamp on a subset of the Northern Anchovy trawl set ( $n = 124$ ). All spectra were collected by technician 1 on the spectrometer at the NOAA-SWFSC La Jolla lab using. The dashed line represents a 1:1 line. The Pearson correlation coefficient ( $r$ ) value is also presented.

### 3.2 Calibration models

Across all species and transformations, the chrome ring *only* model was the best fitting model or performed similarly to the best fitting model, had fewer external variables, and produced absorbance values below 2 AU. Therefore, all calibration models on the full reference set of each species were built from scans using only the chrome ring.

#### *3.2.1 Pacific Sardine*

The chosen calibration model for Pacific Sardine was one with a Savitzky-Golay first derivative with 17 smoothing points (polynomial order = 2) transformation (Table 5; Figure 17). The model with the lowest RMSECV, highest  $R^2$ , and second highest RPD was the model incorporating a Savitzky-Golay first derivative transformation (Table 5) and was chosen as the calibration model for Pacific Sardine (Figure 17). The model incorporating a Savitzky-Golay second derivative transformation yielded almost identical results and could be considered a suitable calibration model as well (Table 5). The calibration model for Pacific Sardine appeared to have limited predictive power (RPD = 2.48, see Section 2.5.2 for explanation on RPD values).

**Table 5.** Partial least squares regression model output for the full Pacific Sardine reference set (n = 537) using a chrome ring only. For the transformations, SNV = Standard normal variate, MSC = Multiplicative scattering correction, SG-1 = Savitzky-Golay first derivative with 17 smoothing points (polynomial order = 2), and SG-2 = Savitzky-Golay second derivative. RMSECV = root mean squared error of cross validation,  $R^2$  = coefficient of multiple determination ( $R^2$ ), RPD = residual prediction deviation.

Transformation	Number of components	RMSECV	$R^2$	RPD
None	6	1.18	0.83	2.46
SNV	6	1.28	0.79	2.31
MSC	6	1.29	0.79	2.31
SG-1	4	1.16	0.83	2.48
SG-2	4	1.19	0.82	2.54

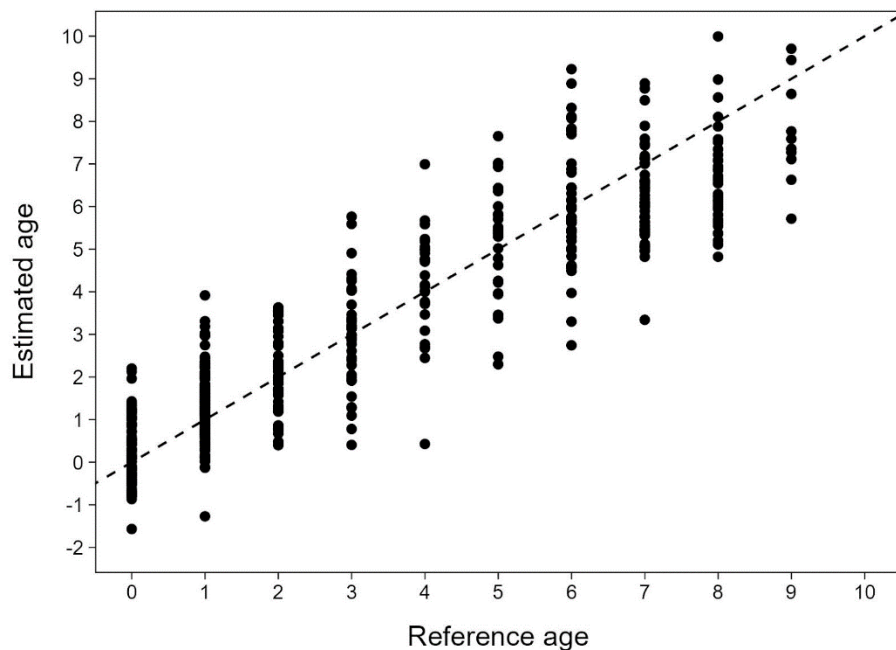


**Figure 17.** Results of the calibration model for Pacific Sardine (n = 537), showing the model estimated ages based on the reference ages determined by traditional ageing. This model incorporated a Savitzky-Golay first derivative transformation. The dashed line represents a 1:1 line.

### 3.2.2 Pacific Mackerel

The model with the lowest RMSECV, highest  $R^2$ , and highest RPD was the model with no transformation, but the model incorporating a Savitzky-Golay first derivative transformation yielded almost identical results (Table 6). The model incorporating a Savitzky-Golay first derivative required a lower number of components compared to the model with no transformation (2 and 4, respectively) and was chosen as the calibration model for Pacific Mackerel (Figure 18). The calibration model for Pacific Mackerel generally had low to no predictive power (RPD = 1.91) and did not appear to perform well for older ages (4+), which was likely due to the small sample sizes for older age classes.

**Table 6.** Partial least squares regression model output for the full Pacific Mackerel reference set ( $n = 278$ ) using a chrome ring only. For the transformations, SNV = Standard normal variate, MSC = Multiplicative scattering correction, SG-1 = Savitzky-Golay first derivative with 17 smoothing points (polynomial order = 2), and SG-2 = Savitzky-Golay second derivative. RMSECV = root mean squared error of cross validation,  $R^2$  = coefficient of multiple determination ( $R^2$ ), RPD = residual prediction deviation.

Transformation	Number of components	RMSECV	$R^2$	RPD
None	4	0.76	0.73	1.99
SNV	5	0.83	0.68	1.86
MSC	4	0.86	0.65	1.76
SG-1	2	0.79	0.71	1.91
SG-2	1	0.80	0.71	1.86

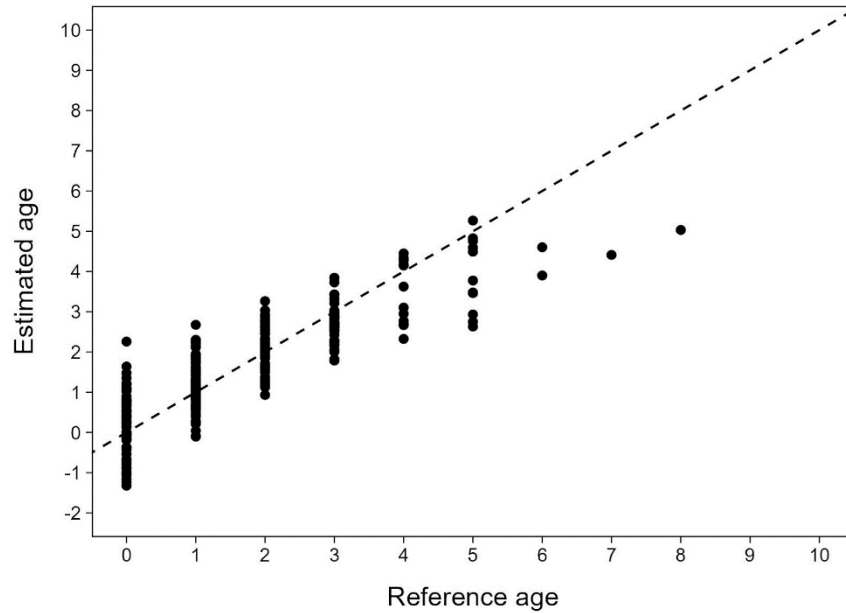


**Figure 18.** Results of the calibration model for Pacific Mackerel ( $n = 278$ ), showing the model estimated ages based on the reference ages determined by traditional ageing. The calibration model for Pacific Mackerel incorporated a Savitzky-Golay first derivative with 17 smoothing points (polynomial order = 2) transformation.

### 3.2.3 Northern Anchovy

The model with the lowest RMSECV, highest  $R^2$ , and highest RPD was the model with a Savitzky-Golay first derivative transformation and was chosen as the calibration model for Northern Anchovy (Table 7; Figure 19). The calibration model for Northern Anchovy had low to no predictive power ( $RPD = 1.89$ ) and did not perform well for older ages (5+), which was likely in part due to the small sample sizes for older age classes, especially ages 6+.

**Table 7.** Partial least squares regression model output for the full Northern Anchovy reference set (n = 332) using a chrome ring only. For the transformations, SNV = Standard normal variate, MSC = Multiplicative scattering correction, SG-1 = Savitzky-Golay first derivative, and SG-2 = Savitzky-Golay second derivative. RMSECV = root mean squared error of cross validation,  $R^2$  = coefficient of multiple determination ( $R^2$ ), RPD = residual prediction deviation.

Transformation	Number of components	RMSECV	$R^2$	RPD
None	5	1.15	0.64	1.74
SNV	4	1.23	0.59	1.62
MSC	4	1.23	0.59	1.62
SG-1	5	1.08	0.69	1.89
SG-2	2	1.20	0.61	1.64

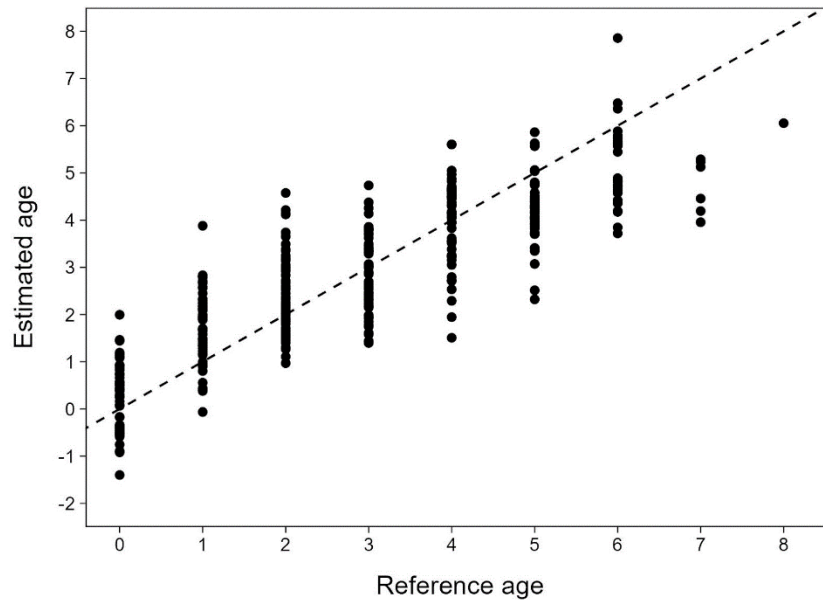


**Figure 19.** Results of the calibration model for Northern Anchovy (n = 332) showing the model estimated ages based on the reference ages determined by traditional ageing. The calibration model for Northern Anchovy incorporated a Savitzky-Golay first derivative with 17 smoothing points (polynomial order = 2) transformation.

#### 4. Discussion

In this study, we developed sample processing and procedures that are best suited to estimate CPS ages from the FT-NIRS methodology using TANGO spectrometers. This study also highlighted major practical challenges that need to be addressed before applying this technology to fish species that are short-lived, fast-growing, and whose otolith sizes (i.e., length and weight) remain small throughout their lifespan. We examined many different variables using both qualitative and quantitative methods to test for differences between processing and procedures used in each of the four experimental trials conducted in this study. For the small pelagic species in this study, we created a protocol that calls for a chrome ring to decrease the size of the quartz window on the spectrometer, and consistent spatial placement of a generally clean, whole otolith on the window. Although not exhaustive, this approach allowed us to consider both practical and analytical issues while selecting the methods that produced the most reproducible and optimal spectral output for CPS.

The premier challenge of using spectral data from otoliths of CPS to estimate age is the small size of CPS otoliths throughout their short life-span. These species complete most of their somatic growth in the first two years of their life, and although their otoliths continue to grow, the amount of  $\text{CaCO}_3$  deposited after they reach 2 years old is relatively small. For example, otoliths of 2-year-old Pacific Sardine, Pacific Mackerel, and Northern Anchovy weigh on average 1.51 mg, 3.44 mg, and 3.40 mg, respectively, whereas otoliths of 5-year-old fish for each species measured on average 2.41 mg, 6.67 mg, and 4.67 mg, respectively (this study). As FT-NIRS spectra record changes in the amount and type of proteins deposited across the otolith, the lack of growth after 2-years may therefore reduce the accuracy of discriminating spectra by CPS age class. Likewise, this issue may not be directly related to the size of the otoliths themselves, but more likely to the rate of increment deposition in CPS otoliths over a given time period. Additionally, due to a short life span, the acceptable error in age estimation may be reduced for species with a 6 to 12-year life span compared to a species with a 30-year lifespan. One other factor is that Pacific Sardine, Pacific Mackerel, and Northern Anchovy have large overlaps in both body and otolith length-at-age as well as otolith weight-at-age (Dorval et al., 2015; Schwartzkopf et al., 2023; Snodgrass et al., 2023), which may contribute to the lower accuracy of CPS age estimates from FT-NIRS compared to other species (e.g., Helser et al., 2019a; Passerotti et al., 2020b).

In addition, the small size of CPS otoliths makes it more difficult to consistently place the otoliths at the same exact position on the quartz window of the spectrometer, and we showed that the position of the otolith on the window has a large impact on the resulting spectra (Figure 6). Because the spectrometer measures the amount of reflected light from the otoliths, placing small otoliths at slightly different positions on the window may lead to large differences in absorbance, and therefore in the number of prominent peaks as demonstrated in this study. In Trial 2a, we found no difference between clean left and right otoliths, which is consistent with Robins et al. (2015) findings for Red Snapper otoliths. However, spectral data will vary between these otolith pairs if placed in different positions. Regardless of the provenance or condition of the otoliths, they must be in the same location and position on the quartz window every time to produce consistent spectral data.

Results from this study also confirmed that minimizing the number of accessories can lead to more reproducible spectral data, while reducing the risk of damaging the quartz window and cost for replacing parts. Yet, using no accessory yields unusable outputs for the smallest otoliths. Because of these issues, we found that the gold stamp potentially added unnecessary variability for CPS spectral data, but this may not be true for other species with larger otoliths. For example, Pacific Mackerel seemed to be less sensitive to the choice of accessory compared to Pacific Sardine and Northern Anchovy, which may be due to their slightly larger otolith sizes. Different technicians using the same machine had the same spectral output, which is promising for long-term precision. Overall, consistency in accessory use coupled with the minimization of variability within and between technicians, instruments, and laboratories appeared to be the key controlling factors in producing reliable FT-NIRS data for small CPS.

One important aspect for using FT-NIRS to predict fish ages is that the accuracy of the calibration model can only be as good as the reference ages provided. Traditionally ageing CPS is known to be difficult and ageing errors (i.e., precision, bias) may vary by age and reader (Kuriyama et al., 2020; Kuriyama et al., 2022; Kuriyama et al., 2023). We chose otoliths for the reference set where all readers agreed upon the age to try to mitigate for any potential biases, but the true (expected) age may not always match the age estimated by readers, particularly for difficult otoliths, especially older individuals; the only example where true and expected age matched was for the Pacific Sardine otoliths marked with OTC.

Determining if each calibration model will perform well on new, unseen data is the next step as any calibration model needs to be validated by predicting the ages of a set of ‘unknown age’ otoliths using the same methodology, and any model should be optimized using variable selection (e.g., using jack-knifed p-values; Goldstein et al., 2021). Once the calibration model is validated, a final prediction model can be determined and then we will be able to evaluate the accuracy of the FT-NIRS method in predicting traditional CPS ages, and whether this methodology could be used to estimate ages for CPS stock assessments. One other avenue of research for using FT-NIRS to age CPS is temporal stability. Otolith chemical composition may change due to environmental and intrinsic factors during long-term storage (Robins et al., 2015), and spectral data from fresh otoliths should be added monthly to assess how long otoliths take to stabilize to produce an identical spectral output each time.

In conclusion, this work represents a large investment of time into research and development of FT-NIRS for CPS, but more work still needs to be done to determine the feasibility of using FT-NIRS to age CPS and other short-lived and fast-growing species, including tradeoffs with traditional ageing methods. Therefore, the method developed in this study may not be the ideal solution for all species with small otoliths, but hopefully provides a blueprint for future species-specific method development.

## **5. Acknowledgements**

We would like to thank Jordan Healy, Morgan Arrington, and Esther Goldstein for their help with the initial R code. We would also like to thank Tom Helser, Irina Benson, Brenna Groom, Michelle Passerotti, Andy Ostrowski, Jamie Clark, Beverly Barnett, Melissa Monk, Jessica Choi, Alexander Rubin, and other members of the NOAA FT-NIRS Strategic Initiative Development Team for their problem-solving and discussions. Thank you to Kelsey James and all the SWFSC, CDFW, and WDFW agers. We are indebted to Jason Erikson from Bruker for all his help with problem solving of the TANGO. We also thank Michelle Passerotti, Esther Goldstein, John Ugoretz, Michelle Horeczko, Brad Erisman, and Annie Yau for their reviews of this manuscript. This work was funded by a NOAA Strategic Initiative.

## 6. References

- Allen, L. G., I. Pondella, D.J., and M. H. Horn. 2006. The ecology of marine fishes: California and adjacent waters, University of California Press, Berkeley.
- Arrington, M. B., T. E. Helser, I. M. Benson, T. E. Essington, M. E. Matta, and A. E. Punt. 2022. Rapid age estimation of longnose skate (*Raja rhina*) vertebrae using near-infrared spectroscopy. *Mar. Freshw. Res.* 73:71-80. 10.1071/Mf21054.
- Baxter, J. L. 1967. Summary of biological information on the northern anchovy, *Engraulis mordax* Girard. *Calif. Coop. Ocean. Fish. Invest. Rep.* 11:110-116.
- Beamish, R. J., and G. A. McFarlane. 1995. A discussion of the importance of aging errors, and an application to walleye pollock: The world's largest fishery. *Recent Developments in Fish Otolith Research* 545-565.
- Beckman, D., and C. A. Wilson. 1995. Seasonal timing of opaque zone formation in fish otoliths. *In* *Recent Developments in Fish Otolith Research* (D. H. Secor, J. M. Dean, and S. E. Campana, eds.), p. 27-43. University of South Carolina Press 19, Columbia, SC.
- Begg, G. A., S. E. Campana, A. J. Fowler, and I. M. Suthers. 2005. Otolith research and application: current directions in innovation and implementation. *Mar. Freshw. Res.* 56:477-483. 10.1071/Mf05111.
- Beleites, C., and V. Sergo. 2023. hyperSpec: a package to handle hyperspectral data sets in R. R package, version 0.100.0 <https://github.com/r-hyperspec/hyperSpec>
- Benson, I. M., T. E. Helser, G. Marchetti, and B. K. Barnett. 2023. The future of fish age estimation: deep machine learning coupled with Fourier transform near-infrared spectroscopy of otoliths. *Can. J. Fish. Aquat. Sci.* 80:1482-1494. 10.1139/cjfas-2023-0045.
- Bertignac, M., and H. de Pontual. 2007. Consequences of bias in age estimation on assessment of the northern stock of European hake (*Merluccius merluccius*) and on management advice. *ICES J. Mar. Sci.* 64:981-988. 10.1093/icesjms/fsm039.
- Campana, S. E., and J. D. Neilson. 1985. Microstructure of fish otoliths. *Can. J. Fish. Aquat. Sci.* 42:1014-1032. DOI 10.1139/f85-127.
- Campana, S. E. 1999. Chemistry and composition of fish otoliths: pathways, mechanisms and applications. *Mar. Ecol. Prog. Ser.* 188:263-297. DOI 10.3354/meps188263.

- Campana, S. E., and S. R. Thorrold. 2001. Otoliths, increments, and elements: keys to a comprehensive understanding of fish populations? *Can. J. Fish. Aquat. Sci.* 58:30-38. DOI 10.1139/cjfas-58-1-30.
- Chang, M. Y., and A. J. Geffen. 2013. Taxonomic and geographic influences on fish otolith microchemistry. *Fish and Fisheries* 14:458-492. 10.1111/j.1467-2979.2012.00482.x.
- Cohen, M., R. S. Mylavarapu, I. Bogrekci, W. S. Lee, and M. W. Clark. 2007. Reflectance spectroscopy for routine agronomic soil analyses. *Soil Science* 172:469-485. 10.1097/ss.0b013e31804fa202.
- Collins, R. A., and J. D. Spratt. 1969. Age determination of northern anchovies, *Engraulis mordax*, from otoliths. *Calif. Fish Game Bull.* 147:39-55.
- D'Acqui, L. P., A. Pucci, and L. J. Janik. 2010. Soil properties prediction of western Mediterranean islands with similar climatic environments by means of mid-infrared diffuse reflectance spectroscopy. *European Journal of Soil Science* 61:865-876. 10.1111/j.1365-2389.2010.01301.x.
- Dahl, K., J. 'Malley, B. Barnett, B. Kline, and J. Widdrington. 2024. Otolith morphometry and Fourier transform near-infrared (FT-NIR) spectroscopy as tools to discriminate archived otoliths of newly detected cryptic species, *Etelis carbunculus* and *Etelis boweni*. *Fish. Res.* 272:106927. 10.1016/j.fishres.2023.106927.
- Dorval, E., J. D. McDaniel, D. L. Porzio, R. Felix-Uraga, V. Hodes, and S. Rosenfield. 2013. Computing and selecting ageing errors to include in stock assessment models of Pacific sardine (*Sardinops sagax*). *Calif. Coop. Ocean. Fish. Invest. Rep.* 54:192-204.
- Dorval, E., J. D. McDaniel, B. J. Macewicz, and D. L. Porzio. 2015. Changes in growth and maturation parameters of Pacific sardine *Sardinops sagax* collected off California during a period of stock recovery from 1994 to 2010. *J. Fish Biol.* 87:286-310. 10.1111/jfb.12718.
- Dorval, E., D. Porzio, B. D. Schwartzkopf, K. C. James, L. Vasquez, and B. Erisman. 2022. Sampling methodology for estimating life history parameters of coastal pelagic species along the U.S. Pacific Coast. NOAA Tech. Memo. NMFS-SWFSC-660, 46 p.
- Eschmeyer, W. N., H. E.S., and H. Hammann. 1983. *A Field Guide to Pacific Coast Fishes of North America from the Gulf of Alaska to Baja California*, Houghton Mifflin Compnay, Boston.

- Fitch, J. E. 1951. Age composition of the southern California catch of Pacific Mackerel 1939–40 through 1950–51. *Calif. Fish Game Bull.* 83:1-73.
- Francis, R. I. C. C. 2016. Growth in age-structured stock assessment models. *Fish. Res.* 180:77-86. 10.1016/j.fishres.2015.02.018.
- Goldstein, E. D., T. E. Helser, J. J. Vollenweider, A. Sreenivasan, and F. F. Sewall. 2021. Rapid and reliable assessment of fish biological condition for fisheries research and management using Fourier Transform Near-Infrared Spectroscopy. *Front. Mar. Sci.* 8:690934.
- Hampton, K. A., A. G. Cavinato, D. M. Mayes, S. J. Boe, and T. L. Hoffnagle. 2002. Near infrared spectroscopic classification of gender and maturity in Chinook salmon (*Oncorhynchus tshawytscha*). *Eastern Oregon Science Journal* 31-36.
- Healy, J., T. E. Helser, I. M. Benson, and L. Tornabene. 2021. Aging Pacific cod (*Gadus macrocephalus*) from otoliths using Fourier-transformed near-infrared spectroscopy. *Ecosphere* 12:ARTN e03697  
10.1002/ecs2.3697.
- Helser, T. E., I. Benson, J. Erickson, J. Healy, C. Kestelle, and J. A. Short. 2019a. A transformative approach to ageing fish otoliths using Fourier transform near infrared spectroscopy: a case study of eastern Bering Sea walleye pollock (*Gadus chalcogrammus*). *Can. J. Fish. Aquat. Sci.* 76:780-789. 10.1139/cjfas-2018-0112.
- Helser, T. E., I. M. Benson, and B. K. Barnett 2019b. Proceedings of the research workshop on the rapid estimation of fish age using Fourier Transform Near Infrared Spectroscopy (FT-NIRS). . *In Book Proceedings of the research workshop on the rapid estimation of fish age using Fourier Transform Near Infrared Spectroscopy (FT-NIRS)*. (Editor, ed.)^eds.), p. 195. City.
- Hilborn, R., and C. J. Walters. 1992. *Quantitative Fisheries Stock Assessment: Choice, Dynamics and Uncertainty*, Chapman and Hall, New York.
- Hüssy, K., H. Mosegaard, and F. Jessen. 2004. Effect of age and temperature on amino acid composition and the content of different protein types of juvenile Atlantic cod (*Gadus morhua*) otoliths. *Can. J. Fish. Aquat. Sci.* 61:1012-1020. 10.1139/F04-037.
- James, K. C., E. Dorval, and B. E. Erisman. *In Review*. Validation of Pacific Sardine (*Sardinops sagax*) annuli from a captive growth experiment. *Marine Biology*.

- Koehn, L. E., T. E. Essington, K. N. Marshall, W. J. Sydeman, A. I. Szoboszlai, and J. A. Thayer. 2017. Trade-offs between forage fish fisheries and their predators in the California Current. *ICES J. Mar. Sci.* 74:2448-2458.  
<https://doi.org/10.1093/icesjms/fsx072>.
- Kucheryavskiy, S. 2020. mdatools: R package for chemometrics. *Chemometrics and Intelligent Laboratory Systems* 198:1-10.
- Kuriyama, P. T., J. P. Zwolinski, K. T. Hill, and P. R. Crone. 2020. Assessment of the Pacific sardine resource in 2020 for U.S. management in 2020-2021. NOAA Tech. Memo. 171 p.
- Kuriyama, P. T., J. P. Zwolinski, S. L. H. Teo, and K. T. Hill. 2022. Assessment of the northern anchovy (*Engraulis mordax*) central subpopulation in 2021 for U.S. management. NOAA Tech. Memo. 114 p.
- Kuriyama, P. T., J. P. Zwolinski, C. Allen Akselrud, and K. T. Hill. 2023. Assessment of Pacific mackerel (*Scomber japonicus*) for U.S. management in the 2023-24 and 2024-25 fishing years. NOAA Tech. Memo. 123 p.
- Lambert, G., T. E. Helser, A. Berger, E. Olsen, J. Hastie, J. O. O'Malley, K. Siegfried, P. Hulson, R. McBride, S. Calay, S. Turner, T. Miller, A. Hollowed, D. Elias, D. Anderl, E. Robillard, J. Short, P. Lynch, and R. D. Methot. 2017. Importance of age data collection for stock assessments: a U.S. national perspective. Report from the Otolith Sampling Size Working Group (OSSWG). NOAA Tech. Memo.
- Liland, K., B. Mevik, and R. Wehrens. 2022. pls: Partial Least Squares and Principal Component Regression. R package, version 2.8-1 <https://CRAN.R-project.org/package=pls>
- Lowenstein, O. 1936. The equilibrium function of the vertebrate labyrinth. *Biological Review of the Cambridge Philosophical Society* 11:113-145.
- McFarlane, G. A., J. Schweigert, L. MacDougall, and C. Hrabok. 2005. Distribution and biology of Pacific sardines (*Sardinops sagax*) off British Columbia, Canada. *Calif. Coop. Ocean. Fish. Invest. Rep.* 46:144-160.
- Methot Jr., R. D., C. R. Wetzel, I. G. Taylor, K. L. Doering, E. G. Gugliotti, and K. F. Johnson. 2023. Stock synthesis user manual, version 3.30.33. . NOAA Fisheries, Seattle, WA.
- Methot, R. D., and C. R. Wetzel. 2013. Stock synthesis: A biological and statistical framework for fish stock assessment and fishery management. *Fish. Res.* 142:86-99.  
[10.1016/j.fishres.2012.10.012](https://doi.org/10.1016/j.fishres.2012.10.012).

- Murayama, E., Y. Takagi, T. Ohira, J. G. Davis, M. I. Greene, and H. Nagasawa. 2002. Fish otolith contains a unique structural protein, otolin-1. *European Journal of Biochemistry* 269:688-696. DOI 10.1046/j.0014-2956.2001.02701.x.
- Passerotti, M. S., T. E. Helser, I. M. Benson, B. K. Barnett, J. C. Ballenger, W. J. Buble, M. J. M. Reichert, and J. M. Quattro. 2020a. Age estimation of red snapper (*Lutjanus campechanus*) using FT-NIR spectroscopy: feasibility of application to production ageing for management. *ICES J. Mar. Sci.* 77:2144-2156. 10.1093/icesjms/fsaa131.
- Passerotti, M. S., C. M. Jones, C. E. Swanson, and J. M. Quattro. 2020b. Fourier-transform near infrared spectroscopy (FT-NIRS) rapidly and non-destructively predicts daily age and growth in otoliths of juvenile red snapper *Lutjanus campechanus* (Poey, 1860). *Fish. Res.* 223:105439. 10.1016/j.fishres.2019.105439.
- Passerotti, M. S., M. J. M. Reichert, B. A. Roberatory, Z. Marsh, M. Stefik, and J. M. Quattro. 2022. Physicochemical mechanisms of FT-NIRS age prediction in fish otoliths. *Mar. Freshw. Res.* 73:846-865. 10.1071/Mf21341.
- Payan, P., H. De Pontual, G. Boeuf, and N. Mayer-Gostan. 2004. Endolymph chemistry and otolith growth in fish. *Comptes Rendus Palevol* 3:535-547. 10.1016/j.crpv.2004.07.013.
- PFMC (Pacific Fishery Management Council). 2019. Coastal Pelagic Species Fishery Management Plan as Amended through Amendment 17.
- PFMC (Pacific Fishery Management Council). 2022. Status of the Pacific coast coastal pelagic species fishery and recommended acceptable biological catches. Stock Assessment and Fishery Evaluation 2021 including information through June 2021.
- R Core Team. 2022. R: A language and environment for statistical computing. R Foundation for Statistical Computing, Vienna, Austria. <https://www.R-project.org/>
- Rasco, B. A., C. E. Miller, and T. L. King. 1991. Utilisation of NIR spectroscopy to estimate the proximate composition of trout muscle with minimal sample pre-treatment. *Journal of Agriculture and Food Chemistry* 39:67-72.
- Reeves, S. A. 2003. A simulation study of the implications of age-reading errors for stock assessment and management advice. *ICES J. Mar. Sci.* 60:314-328. [https://doi.org/10.1016/S1054-3139\(03\)00011-0](https://doi.org/10.1016/S1054-3139(03)00011-0).
- Robins, J. B., B. B. Wedding, C. Wright, S. Grauf, M. Sellin, A. Fowler, and T. Saunders. 2015. Revolutionising Fish Ageing: Using Near Infrared Spectroscopy to Age Fish. *The*

- Fisheries Research and Development Corporation and The State of Queensland (through the Department of Agriculture and Fisheries).
- Schober, P., C. Boer, and L. A. Schwarte. 2018. Correlation coefficients: appropriate use and interpretation. *Anesthesia and Analgesia* 126:1763-1768.  
10.1213/Ane.0000000000002864.
- Schwartzkopf, B. D., E. Dorval, K. C. James, J. M. Walker, O. E. Snodgrass, D. L. Porzio, and B. E. Erisman. 2022. A summary report on life history information on the central subpopulation of Northern Anchovy (*Engraulis mordax*) for the 2021 stock assessment. NOAA Tech. Memo. NOAA-SWFSC-659, 76 p.
- Schwartzkopf, B. D., E. Dorval, D. L. Porzio, J. M. Walker, K. C. James, and B. E. Erisman. 2023. Modeling somatic and otolith growth of the central subpopulation of northern anchovy. by incorporating seasonality. *Fish. Bull.* 121:172-187. 10.7755/Fb.121.4.3.
- Secor, D. H., J. M. Dean, and E. H. Laban. 1992. Otolith removal and preparation for microstructural analysis. *In* Otolith micro-structure examination and analysis (D. K. Stevenson, and S. E. Campana, eds.), p. 19-57. Department of Fisheries and Oceans Canadian Special Publication of Fisheries and Aquatic Sciences, Ottawa.
- Secor, D. H., J. M. Dean, and S. E. Campana. 1995. Recent Developments in Fish Otolith Research, University of South Carolina Press, Columbia.
- Siskey, M. R., A. E. Punt, P. J. F. Hulson, M. D. Bryan, J. N. Ianelli, and J. T. Thorson. 2023. The estimated impact of changes to otolith field-sampling and ageing effort on stock assessment inputs, outputs, and catch advice. *Can. J. Fish. Aquat. Sci.* 80:115-131.  
10.1139/cjfas-2022-0050.
- Snodgrass, O. E., E. Dorval, K. C. James, B. D. Schwartzkopf, J. M. Walker, D. L. Porzio, B. J. Macewicz, and B. E. Erisman. 2023. A summary report of life history information on Pacific Mackerel (*Scomber japonicus*) for the 2023 stock assessment. NOAA Tech. Memo. XXX p.
- Sohn, D., S. Kang, and S. Kim. 2005. Stock identification of chum salmon (*Oncorhynchus keta*) using trace elements in otoliths. *Journal of Oceanography* 61:305-312. DOI 10.1007/s10872-005-0041-3.
- Sorvaniemi, J., A. Kinnunen, A. Tsados, and Y. Malkki. 1993. Using partial least-squares regression and multiplicative scatter correction for FT-NIR data evaluation of wheat

- flours. Food Science and Technology-Lebensmittel-Wissenschaft & Technologie 26:251-258.
- Thomas, O. R. B., K. L. Richards, S. Petrou, B. R. Roberts, and S. E. Swearer. 2020. In situ 3D visualization of biomineralization matrix proteins. Journal of Structural Biology 209:107448. doi:10.1016/j.jsb.2020.107448.
- Thompson, A. R., I. D. Schroeder, S. J. Bograd, E. L. Hazen, M. G. Jacox, A. Leising, B. K. Wells, J. L. Largier, J. L. Fisher, K. Jacobson, S. Zeman, E. P. Bjorkstedt, R. R. Robertson, M. Kahru, R. Goericke, C. E. Peabody, T. R. Baumgartner, B. E. Lavaniegos, L. E. Miranda, E. Gomez-Ocampo, J. Gomez-Valdes, T. D. Auth, E. A. Daly, C. A. Morgan, B. J. Burke, J. C. Field, K. M. Sakuma, E. D. Weber, W. Watson, J. M. Porquez, J. Dolliver, D. E. Lyons, R. A. Orben, J. E. Zamon, P. Warzybok, J. Jahncke, J. A. Santora, S. A. Thompson, B. Hoover, W. Sydeman, and S. R. Melin. 2019. State of the California Current 2018–19: A novel anchovy regime and a new marine heat wave? Calif. Coop. Ocean. Fish. Invest. Rep. 60:1-65.
- Wedding, B. B., A. J. Forrest, C. Wright, S. Grauf, P. Exley, and S. E. Poole. 2014. A novel method for the age estimation of Saddletail snapper (*Lutjanus malabaricus*) using Fourier Transform-near infrared (FT-NIR) spectroscopy. Mar. Freshw. Res. 65:894-900.
- Weigele, J., T. A. Franz-Odenaal, and R. Hilbig. 2016. Not all inner ears are the same: otolith matrix proteins in the inner ear of sub-adult cichlid fish, *Oreochromis mossambicus*, reveal insights into the biomineralization process. The Anatomical Record 299:234-245.
- Wolf, R. S., and A. E. Daugherty. 1961. Age and length composition of the sardine catch off the Pacific coast of the United States and Mexico in 1958-59. Calif. Fish Game Bull. 46:2630275.
- Wright, C., B. B. Wedding, S. Grauf, and O. J. Whybird. 2021. Age estimation of barramundi (*Lates calcarifer*) over multiple seasons from the southern Gulf of Carpentaria using FT-NIRS spectroscopy. Mar. Freshw. Res. 2.
- Yaremko, M. L. 1996. Age determination in Pacific sardine, *Sardinops sagax*. NOAA-SWFSC-223, 38 p.
- Yule, D. L., J. D. Stockwell, J. A. Black, K. I. Cullis, G. A. Cholwek, and J. T. Myers. 2008. How systematic age underestimation can impede understanding of fish population

dynamics: Lessons learned from a Lake Superior cisco stock. *Trans. Am. Fish. Soc.* 137:481-495. 10.1577/T07-068.1.

Zwolinski, J. P., and D. A. Demer. 2023. An updated model of potential habitat for northern stock Pacific Sardine (*Sardinops sagax*) and its use for attributing survey observations and fishery landings. *Fish. Oceanogr.* <https://doi.org/10.1111/fog.12664>.